

CONTRIBUTIONS FROM THE MUSEUM OF PALEONTOLOGY

THE UNIVERSITY OF MICHIGAN

VOL. 30, NO. 11, PP. 269-319

December 31, 2001

**EOCENE STRATIGRAPHY AND ARCHAEOCETE WHALES
(MAMMALIA, CETACEA) OF DRUG LAHAR IN THE
EASTERN SULAIMAN RANGE, BALOCHISTAN (PAKISTAN)**

BY

PHILIP D. GINGERICH, MUNIR UL-HAQ, INTIZAR HUSSAIN KHAN,
AND IYAD S. ZALMOUT



MUSEUM OF PALEONTOLOGY
THE UNIVERSITY OF MICHIGAN
ANN ARBOR

CONTRIBUTIONS FROM THE MUSEUM OF PALEONTOLOGY

Philip D. Gingerich, Director

This series of contributions from the Museum of Paleontology is a medium for publication of papers based chiefly on collections in the Museum. When the number of pages issued is sufficient to make a volume, a title page plus a table of contents will be sent to libraries on the Museum's mailing list. This will be sent to individuals on request. A list of the separate issues may also be obtained by request. Correspondence should be directed to the Publications Secretary, Museum of Paleontology, The University of Michigan, 1109 Geddes Road, Ann Arbor, Michigan 48109-1079.

VOLS. 2-30: Parts of volumes may be obtained if available. Price lists are available upon inquiry.

Text and illustrations ©2001 by the Museum of Paleontology, University of Michigan

**EOCENE STRATIGRAPHY AND ARCHAEOCETE WHALES
(MAMMALIA, CETACEA) OF DRUG LAHAR IN THE
EASTERN SULAIMAN RANGE, BALOCHISTAN (PAKISTAN)**

BY

PHILIP D. GINGERICH¹, MUNIR UL-HAQ², INTIZAR HUSSAIN KHAN³,
AND IYAD S. ZALMOUT¹

Abstract — Field work in autumn 1999 was concentrated in marine middle and upper Eocene strata of Dabh Nala, a tributary of Drug Lahar, on the eastern flank of the Sulaiman Range, Balochistan Province, Pakistan. Objectives included: (1) recovery of better specimens of previously-known archaeocete whales; (2) recovery of new archaeocetes from new stratigraphic intervals; (3) comparison of Eocene formations here with those studied elsewhere in Balochistan and Punjab; and (4) better documentation of local and regional sea level cycles for refined correlation to eustasy on a global scale.

Ten stratigraphic intervals within the Habib Rahi and Domanda formations are now known to yield archaeocetes. These come from three distinct cycles of sea level rise and fall. Interpretation in the context of planktonic foraminiferal and nannoplankton age control for a virtually continuous Baska-Habib Rahi-Domanda-Pir Koh-Drazinda stratigraphic section shows that the Habib Rahi through Domanda cycles match the global pattern of sea level change for the Lutetian. Archaeocete-bearing strata of the Harudi Formation in Kutch (India) are early Bartonian rather than Lutetian, and correlative with the Pir Koh flooding event in Pakistan.

New archaeocete specimens described here include the first record of the remingtonocetid *Andrewsiphium sloani*, new combination, from the upper Domanda Formation (late Lutetian in age); a new species of *Remingtonocetus*, *R. domandaensis*, based on a partial skull, a dentary with most teeth, and associated postcranials, from the middle Domanda Formation (middle Lutetian); and a new genus and species of protocetid, *Qaisracetus arifi*, based on a partial skull and unusually complete articulated axial skeleton from the upper Domanda Formation (late Lutetian).

INTRODUCTION

The Sulaiman Range is a north-south trending band of rugged mountains rising 1,000 to 3,400 m (11,000 ft) above sea level that defines the modern political boundary between Balochistan and

¹Museum of Paleontology and Department of Geological Sciences, The University of Michigan, Ann Arbor, Michigan 48109-1079

²Paleontology and Stratigraphy Branch, Geological Survey of Pakistan, Sariab Road, Quetta

³Technical Directorate, Geological Survey of Pakistan, Sariab Road, Quetta

Punjab provinces, and extends northward into North-West Frontier Province (Fig. 1). Late Mesozoic and Cenozoic sedimentary rocks here are predominantly marine and accumulated in the Tethys Sea in what is now the Indus Basin, bounded to the northwest by the Axial Belt (Shah, 1977) or Bela-Waziristan Ophiolite Zone (Bannert et al., 1992), and to the southeast by the Indo-Pakistan Subcontinent. Indo-Pakistan was located astride the equator in Eocene time, moving northward toward tectonic collision with the rest of Asia (Patriat and Achache, 1984). The east side of the Sulaiman Range has a thick sequence of lower, middle, and upper Eocene sedimentary rocks, well exposed today, that were deposited on a shallow shelf on the leading edge of the subcontinent before closure of Tethys and suturing to the rest of Asia. The middle and upper part of this stratigraphic sequence, the Kirthar or Kirthar-equivalent group comprising the Habib Rahi, Domanda, Pir Koh, and Drazinda formations (Shah, 1991), is of particular interest as one of the richest archaeocete whale-bearing intervals known anywhere in the world.

The first fossil mammals from this area were described by Pilgrim (1940) from what is now called Domanda Formation (Hemphill and Kidwai, 1973; Shah, 1991). Pilgrim described a small collection interpreted as land mammals and reptiles from the 'Lower Kirthar shales' of Safed Tobah (29° 25' N latitude, 69° 57' E longitude), on the eastern flank of the Sulaiman range in Rajanpur District, Punjab Province. The land mammals were attributed to Mesonychidae (*Condylarthra*) and *Anthracotheroidea* (*Artiodactyla*), and the reptiles were attributed to *Crocodylia* and *Chelonina* (Pilgrim, 1940). Field work in 1977 established that the Domanda Formation at Rakhi Nala (29° 56.5' N, 70° 07' E), some 60 km north of Safed Tobah, is entirely marine, although it yielded sacral vertebrae and pieces of innominate attributed to land mammals (Gingerich et al., 1979). Subsequent study of Pilgrim's 'land mammals' and 'reptiles' in the Natural History Museum, London, and of 'land mammals' in our 1977 collection has shown that most are remains of archaeocete cetaceans.

Rakhi Nala is the classic Eocene section of western Punjab described by Eames (1951, 1952a-c), and studied by Latif (1964), Siddiqui (1971), Samanta (1973), Köthe et al. (1988), Afzal (1996), Warraich et al. (2000), and others. A Geological Survey of Pakistan-University of Michigan [GSP-UM] expedition to Rakhi Nala in 1981, following up on the archaeocetes recovered previously, yielded one partial skeleton of a primitive protocetid from the Habib Rahi Formation (Wells, 1984; Gingerich, 1991), and one remingtonocetid and two protocetid specimens from the Domanda Formation (Wells, 1984; Gingerich et al., 1993, 1995a).

With this background, we restarted field work in the Domanda Formation in 1992. Our efforts were concentrated near Satta in the northern plunge of the Zinda Pir anticlinorium where dips are relatively shallow (ca. 30°) and hence advantageous for collecting fossils. This area yielded remingtonocetid and protocetid remains (Gingerich et al., 1993), most notably the skull and partial skeleton of *Rodhocetus kasranii*¹ (Gingerich et al., 1994). Stratigraphic sections measured in the northern plunge were unsatisfactory because we were unable to find an area where the thicknesses of shales could be measured confidently.

In 1994 we worked in Rakhi Nala measuring stratigraphic sections and taking paleomagnetic samples from the entire Kirthar group of formations (Habib Rahi, Domanda, Pir Koh, and Drazinda) in an attempt to improve correlation to the global geological time scale. This attempt at correlation proved only partially successful (Gingerich et al., 1995b, 1998), and was misleading until integrated with the available biostratigraphy (Gingerich et al., 1997). The remainder of the 1994 field season was spent prospecting in the Domanda Formation at Takra in the southern plunge of the Zinda Pir anticlinorium, where we found a skull and partial skeleton of a new remingtonocetid, *Dalanistes ahmedi*, and skulls of two new protocetids, *Takracetus simus* and *Gaviacetus razai* (Gingerich et al., 1995a). Our measured stratigraphic sections confirmed that the Domanda Formation is some 300 m thick in the Rakhi Nala area, while it is only about 240 m thick in the Takra area. We divided the Domanda Formation into lower, middle, and upper parts, but these initial subdivisions require revision (see below).

¹The original specific name *kasrani* is amended to *kasranii* here, adding an *i* to correctly reflect commemoration. The species is named for the Kasrani Baloch tribe inhabiting western Punjab and easternmost Balochistan. Authorship dates to the original publication by Gingerich et al. (1994).

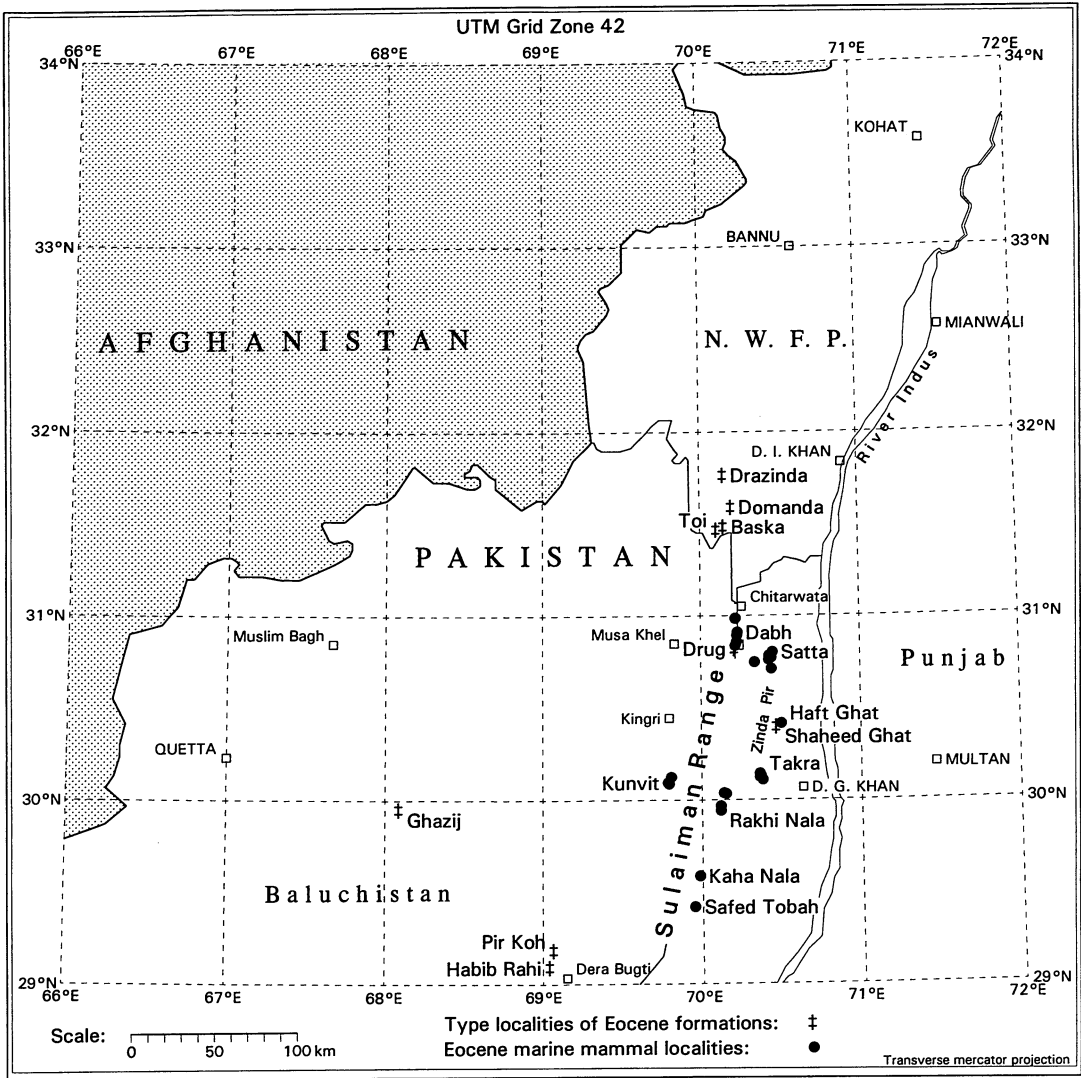


FIG. 1 — Location map showing the Drug and Dabh area of interest here, at the easternmost edge of Balochistan Province (at 30° 55' N latitude and 70° 13' E longitude). Type localities of Eocene formations discussed in the text are marked with a double-dagger symbol. Geological Survey of Pakistan-University of Michigan localities yielding Eocene marine mammals in eastern Balochistan and western Punjab are marked with solid circles.

In 1996 we spent several days working in the Domanda Formation at Safed Tobah, revisiting the source of the collection described by Pilgrim (1940). The Domanda there is attractive because satellite images show it to be an area where strata are exposed over a broad area with low dips. We were able to confirm that archaeocetes are reasonably common there, but access is difficult and security problems forced us to leave this area before we found many important specimens. Parts of the remainder of the 1996 field season were spent in the Domanda Formation near both Satta and Takra, where we found a well preserved dentary of *Dalanistes ahmedi*, a well preserved dentary and partial sacrum of *Takracetus simus*, and more of the type specimen, including a nearly complete dentary, of *Gaviacetus razai*. The 1996 Domanda collection will be described as these taxa are restudied.

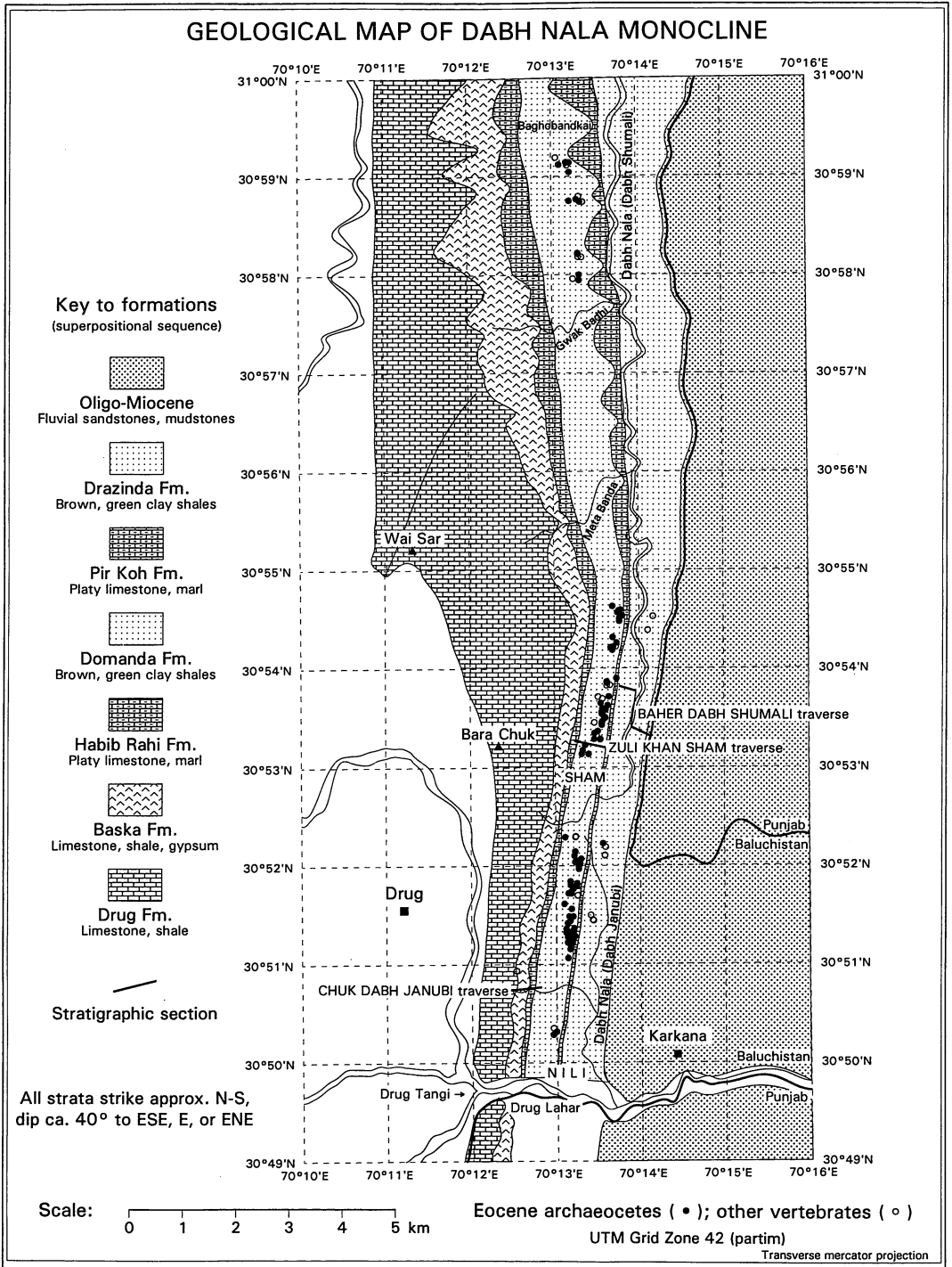


FIG. 2 — Geological map of Dabh Nala monocline, showing the outcrop area of Drug, Baska, Habib Rahi, Domanda, Pir Koh, and Drazinda formations in this part of easternmost Balochistan. Dip of strata averages about 40° downward to the east on the southern part of the map, and slightly less on the northern part of the map. Stippled area at right represents the combined Chitarwata and Vehowa formations of Oligocene and

Another area that satellite imagery shows to be advantageous in having strata broadly exposed with relatively shallow dips borders Drug Lahar in easternmost Balochistan (Fig. 1). We made an initial reconnaissance visit in May of 1999 (when daytime temperatures of 40-45° C precluded any serious field work), and then returned for all of November, 1999. Our objectives included: (1) recovery of better specimens of previously-known archaeocete whales; (2) recovery of new archaeocetes from new stratigraphic intervals; (3) comparison of Eocene formations in the Drug area with those studied elsewhere in Balochistan and Punjab; and (4) better documentation of local and regional sea level rise and fall for refined correlation to the global pattern of sea level change. It turned out that both the Domanda and Drazinda formations are so well exposed here that much more time would be required to survey them adequately. We concentrated virtually all of our effort in 1999 on the Domanda Formation.

ABBREVIATIONS

- GSP-UM — Geological Survey of Pakistan-University of Michigan collection, Quetta (Pakistan)
 LUVF — Lucknow University vertebrate paleontology collection, Lucknow (India)

DRUG LAHAR AND DABH NALA

Drug Lahar is a perennial stream draining the eastern slope of the Sulaiman Range. It is named for the small agricultural settlement of Drug (pronounced *driig*, or *droog*), surrounded on the north and east by a spectacular escarpment of Eocene limestone, the Drug Limestone or Drug Formation (Shah, 1990, 1991). Several tributaries join here before passing through Drug Tangi, a narrow gorge carved through the Drug Limestone. Drug Lahar flows eastward to join Sanghar Lahar and then the Indus River. The particular part of Drug Lahar of interest here is called Dabh Nala, on the dip slope of the Drug Limestone north of Drug Lahar (Fig. 2). This has a well exposed section of the Baska, Habib Rahi, Domanda, Pir Koh, Drazinda and Chitarwata formations.

Dabh is a word in local Baluchi and Peshto dialects meaning 'valley' in some broad generic sense, and, confusingly, many valleys in the Sulaiman Range are named Dabh. As used here, Dabh Nala refers to the long north-south trending lowland north of Drug Lahar that is bordered by a high ridge of Drug Formation Eocene limestones on the west and a high escarpment of Chitarwata Formation Oligo-Miocene sandstones on the east (Fig. 2). The Chitarwata escarpment marks the boundary between Balochistan and Punjab provinces in this area, and hence Dabh Nala lies just within Balochistan. The Dabh region extends from Drug Lahar or river valley near the settlement of Drug in the south (ca. 30° 50' N and 70° 13' E) to Badri Nala or valley near Chitarwata Post in the north (ca. 31° 01' N and 70° 14' E), a distance of some 20 km. Dabh here is not a single valley, but a northern and a southern set of three parallel valleys each, all collectively referred to as Dabh Nala. The three valleys draining to the north into Badri Nala are Baher Dabh Shumali (outer-Dabh north) developed in Drazinda shales, Ander Dabh Shumali (inner-Dabh north) developed in Domanda shales, and Chuk Dabh Shumali (peak-Dabh north) developed in lower Baska shales.

Miocene age. The Drug, the upper Baska plus Habib Rahi, the Pir Koh, and the Chitarwata plus Vehowa formations are resistant to erosion and ridge forming, while the lower Baska, the Domanda, and the Drazinda formations are more readily eroded and thus exposed in intervening valleys. Drug Tangi (gorge) is the type locality of the Drug Formation. Solid lines show the locations of the Chuk Dabh Janubi, Zuli Khan Sham, and Baher Dabh Shumali traverses along which stratigraphic sections described here were measured. Eocene archaeocete specimens found in 1999 are mapped as solid circles, and other vertebrate specimens are mapped as open circles. Solid squares are villages. Solid triangles are topographic peaks.

The three valleys draining to the south into Drug Lahar are Baher Dabh Janubi (outer-Dabh south) developed in Drazinda shales, Ander Dabh Janubi (inner-Dabh south) developed in Domanda shales, and Chuk Dabh Janubi (peak-Dabh south) developed in lower Baska shales. Two of the six nalas are river valleys proper, both developed in Drazinda shales: Baher Dabh Shumali, called Dabh Nala by local people; and Baher Dabh Janubi, labeled Dabh Nala on maps. The inner valleys paralleling these are dissected transversely by tributaries of the principal north and south-draining Dabh nalas. Both outer valleys carry streams originating in a high headland or *sham* called Zuli Khan Sham.

Geologically the Dabh Nala area is a broad monocline striking approximately north-south and dipping toward the east at about 40°. Resistance of different lithologies to erosion controls the development of valleys. The resistant ridges separating individual valleys are, in stratigraphic order from west to east: Drug Formation limestones; upper Baska Formation limestones and massive gypsum beds plus Habib Rahi Formation limestones and marls; Pir Koh Formation limestones and marls; and Chitarwata Formation sandstones. As just noted, the intervening valleys are, in stratigraphic order from west to east: lower Baska Formation shales; Domanda Formation shales; and Drazinda Formation shales.

STRATIGRAPHIC SECTIONS

Stratigraphic sections of the Baska, Habib Rahi, Domanda, Pir Koh, and Drazinda formations were measured in three traverses, one traverse crossing each of the parallel Dabh valleys. Locations of traverses are shown in Figure 2. Sections are drawn to scale in Figures 3, 5, and 9, and full logs for each of the five formations are listed in Appendix tables A-1 through A-5.

The four Kirthar group formations studied here, Habib Rahi, Domanda, Pir Koh, and Drazinda, have been observed in many parts of Dabh Nala and elsewhere, and sections have been measured at Rakhi Nala, Takra, and Satta (Gingerich et al., 1995a, 1997, 1998). Kirthar-group formations are exceptionally well exposed in Dabh Nala. There are minor differences from place to place, but the sections described here are broadly representative of all four formations over much of the north-south trending Sulaiman front.

Stratigraphic sections documented here were measured with a Jacob's staff, with measurements recorded to the nearest centimeter (these are considered to have approximately decimeter precision). A centimeter tape was used to record thicknesses of some of the thinner beds. Each section was measured to quantify the thickness of formations as a whole for comparison with thicknesses reported at type localities (Table 1). Within each formation, the thicknesses, colors, lithologies, and fossil content of successive beds were recorded to identify and place marker horizons, and to facilitate sea level interpretation. Age-diagnostic microfossils are available from some parts of some formations, providing overall temporal control, but high and low sea stands are important for refined correlation to the global sea level curve.

Chuk Dabh Janubi section

The Chuk Dabh Janubi section (Fig. 3) includes the entire 197 m thickness of the Baska Formation named by Hemphill and Kidwai (1973), which is equivalent to the "Shales with Alabaster" described by Eames (1952a) in Rakhi Nala on the east side of the Sulaiman Range farther to the south. The base of the Baska Formation is the top of the underlying Drug Formation, taken as the top of the highest nodular limestone, a 60 cm thick unit exposed as an eastward-dipping planar surface. The Baska Formation lies conformably on top of this. The strike of the Baska Formation at the base of the Chuk Dabh Janubi section is ca. N 8° E, and the dip is ca. 39° ENE. The dip increases to ca. 45° ENE up-section. The lower 100 m or so of the Baska Formation is predominantly composed of fissile shales with interbedded limestones that erode to form a narrow valley (Chuk Dabh) on top of the broad Drug Formation dip slope (Fig. 4). The upper 97 m or so of the

Chuk Dabh Janubi section

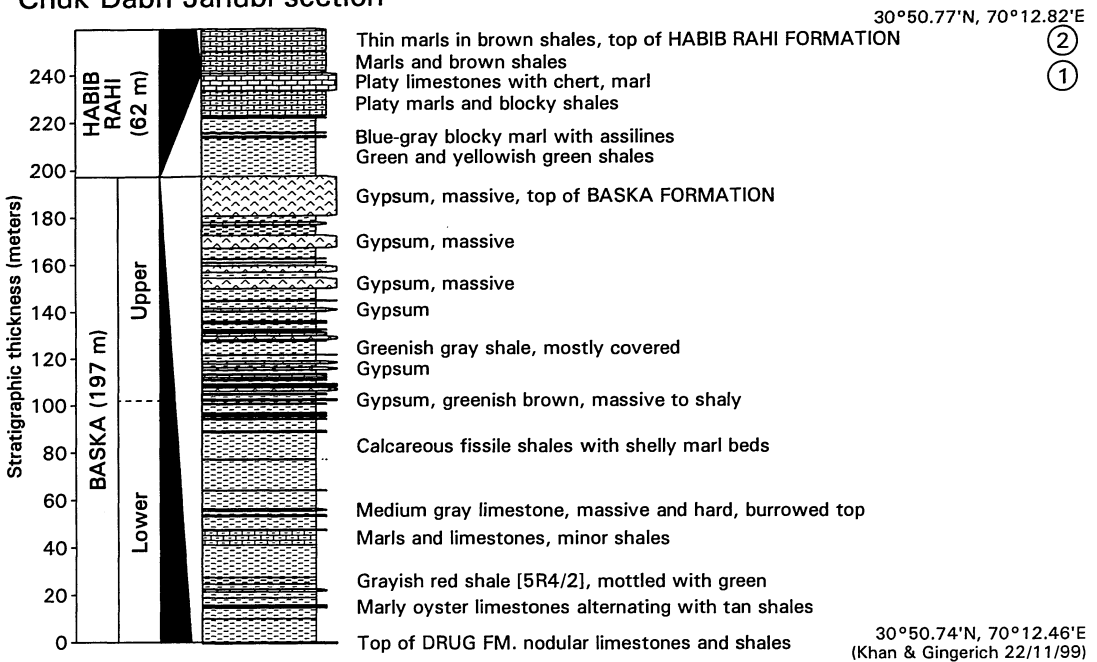


FIG. 3 — Chuk Dabh Janubi stratigraphic section of the 197-m thick Baska Formation and the 62-m thick Habib Rahi Formation. Location of the Chuk Dabh Janubi traverse is shown on the map in Figure 2. There is a 2.8 m thick tongue of grayish red shale 25-28 m above the base of the Baska Formation. The lower part of the formation is shale-rich and valley-forming (Fig. 4). The upper part of the formation is dominated by ridge-forming massive gypsum beds that thicken up-section. Sea level interpretation is shown by the width of the black band in the third column: this is widest during times of high sea stand, and narrowest during times of low sea stand. Section logs for each formation are recorded in Appendix tables A-1 and A-2. Circled numbers at right enumerate known archaeocete-bearing intervals within Lutetian strata of the Sulaiman Range (continued in Fig. 5).

TABLE 1 — Type sections and thicknesses, where known, of Eocene formations exposed on the eastern flank of the Sulaiman Range in Balochistan, North-West Frontier, and Punjab provinces, Pakistan. Thicknesses in Dabh Nala are listed for comparison. Formations are shown in superpositional order. Type localities are plotted graphically in Fig. 1. Asterisks denote estimates.

Formation	Type locality	Latitude	Longitude	Author(s)	Thicknesses (m)	
					Type section	Dabh section
Drazinda	Drazinda village	31°46.00'N	70°09.00'E	Hemphill and Kidwai (1973: 16)	457*	434
Pir Koh	Pir Koh range	29°10.90'N	69°03.80'E	Tainish et al. (1959: 2679)	135	19
Domanda	Domanda Post	31°35.50'N	70°09.00'E	Hemphill and Kidwai, 1973: 16)	305*	366
Habib Rahi	Habib Rahi Nala ¹	29°05.44'N	69°02.35'E	Tainish et al. (1959: 2679)	—	62
Baska	Baska village	31°29.00'N	70°08.00'E	Hemphill and Kidwai (1973: 14)	189	197
Drug	Drug Tangi	30°49.25'N	70°12.50'E	Shah (1990: 71)	400	400*
Shaheed Ghat	Shaheed Ghat	30°24.00'N	70°28.00'E	Shah (1990: 69)	689	600*

¹Location and coordinates of type section of Habib Rahi Formation provided by Shahid Hasan Khan, GSP

Baska Formation contains more numerous limestones and thirteen massive gypsum units that together form a massive north-south trending ridge. All beds are tabular and persistent along



FIG. 4 — Photograph of the lower part of the Baska Formation in the Chuk Dabh Janubi stratigraphic section. This shows the predominance of shale and the tabular nature of interbedded limestones in the lower part of the section. View is to the north, with the bare dip slope of the Drug Formation limestone visible in the left distance. Man at right side of photograph (arrow) is sitting on the meter-thick limestone 56 m above the base of the section.

strike. The Baska Formation has not yielded marine mammals to date, although there is a good possibility that parts of it might in the future.

The Habib Rahi Formation includes the *Assilina* bed of Eames (1952a), and the “Platy Limestone” of La Touche (1893) and Eames (1952a). In the Zuli Khan Sham section it has a total thickness of 62 m and consists of: some 25 m of green shales and assilina-rich marls; 11 m of 30 cm-thick marl beds alternating with 20 cm-thick blocky shales; then 8 m of 15 cm-thick limestones including thin brown and black chert beds that are interbedded with marl and shale; then 9 m of 10 cm-thick marls alternating with 40 cm brown shales; and, finally, 10 m of thin marl beds more widely spaced in a matrix of brown shales (Appendix table A-2). It seems natural to include the transitional green shales and *Assilina* beds as the base of the Platy Limestone or Habib Rahi Formation, as Eames (1952a) and Hemphill and Kidwai (1973) did, because these indicate a return to more normal marine conditions and are undoubtedly the beginning of the major Habib Rahi transgression.

The age of the Baska Formation is reported as late early Eocene by Fritz (in Hemphill and Kidwai, 1973, p. 15), and the age of the Habib Rahi Formation is reported as probably middle Eocene by Hemphill and Kidwai (1973, p. 17), based on limited paleontological evidence available at the time. The Baska Formation is still poorly dated but it is now known to be bracketed by a planktonic foraminiferal P9 age (late Ypresian) for the underlying Drug Formation (Afzal, 1996), and a nannoplankton NP14-15 age (early Lutetian) for the overlying Habib Rahi Formation (Köthe et al., 1988).

Sea level interpretation of the Baska Formation is based on three observations of lithology and lithostratigraphy:

- (1) The underlying 400 m thick Drug Formation is predominantly composed of marine limestone, massively-bedded in the middle part, with thinner nodular limestones separated by shale interbeds in the upper part. This is interpreted as a relatively deep-water sequence, possibly shallowing upward.
- (2) The Baska Formation includes, first, 100 m or so of beds in the lower part with a shale component increasing upward, indicating continental influence; and then 97 m or so of beds in the upper part with a massively-bedded gypsum component increasing upward. The entire formation is interpreted as a shallowing-upward sequence, with the evaporite-rich upper part of the Baska Formation being deposited in a shallow sea of restricted circulation.
- (3) Finally, the Baska Formation is overlain by green shales and assiline-rich marls of the Habib Rahi Formation that give way to a thicker unit of platy limestones with cherts and marl interbeds. The latter is a relatively deep-water facies and indicates renewed flooding.

Intervals of flooding and shallowing interpreted from lithology are shown in the third column of Figure 3, where black predominates during intervals of sea level rise and flooding, and white predominates during intervals of sea level fall and shallowing. A latest Ypresian age for the lower Baska Formation is consistent with the general pattern of sea level change and with planktonic micropaleontological control where this is available (see below).

Zuli Khan Sham section

The Domanda Formation measured in the Zuli Khan Sham traverse is shown in the Zuli Khan Sham section (Fig. 5). It is equivalent to the "Lower Chocolate Clays" of Eames (1952a). These, however, are not nearly so homogeneous as Eames implies. Three distinct cycles of rapid flooding and slower upward shallowing are represented, which are evident in the clear pattern of color change observed in outcrop (Fig. 6). The transition from the underlying Habib Rahi Formation is perfectly gradational, and the boundary is necessarily somewhat arbitrary, assessed on the basis of predominance of limestone and marl versus shale. Platy limestone and marl bands of the Habib Rahi thin upward and are separated by increasing thicknesses of gray-brown to blue-gray shale until the carbonate bands disappear.

Between 74 and 121 m above the base of the Domanda Formation, olive gray and yellowish brown shales are interbedded with several laterally-persistent 20-30 cm thick yellow and orange marl or impure limestone bands (Fig. 5; Appendix table A-3). These are not planar like most limestones here but have an undulating surface and 'ropey' texture. They are sometimes associated with distinctive vertical pillars or pods of marl penetrating through overlying shale and standing as high as a meter above the land surface (Fig. 7A). We have not excavated such pods to see that they connect to the underlying laterally-persistent bands, but flower-like structures in the latter appear to be truncated bases of such pillars or pods (Fig. 7B). One of these pods was illustrated previously as the source of the type specimen of the protocetid *Takracetus simus* (Gingerich et al., 1995a, fig. 5). A second specimen of *T. simus* was found in 1996 weathering out of such a pod near Satta. We interpret these pods as dewatering structures of some kind, or compression extrusions in marl or impure limestone bands that developed when these were compressed by overlying sediment. Conceivably they might have been fed by spring-like sources of brackish or fresh water on the sea floor that might have attracted protocetids.

Some 133 m above the base of the Domanda Formation, gray and yellowish brown shales give way to a 55 m-thick interval of orange- and brown-weathering 'multani' or fuller's earth (Fig. 5; Appendix table A-3). Shales in this interval are generally light olive gray when broken on a fresh surface, but shale partings are dark reddish brown and this addition of color yields the distinctive weathered color. The presence of orange, red, and brown colors in this interval is interpreted as indicating oxidation in a shallower sea, and the 188 m level in the Domanda Formation is taken as the top of the lowest shallowing-upward cycle of sea level change (a cycle that started with the Habib Rahi flooding event).

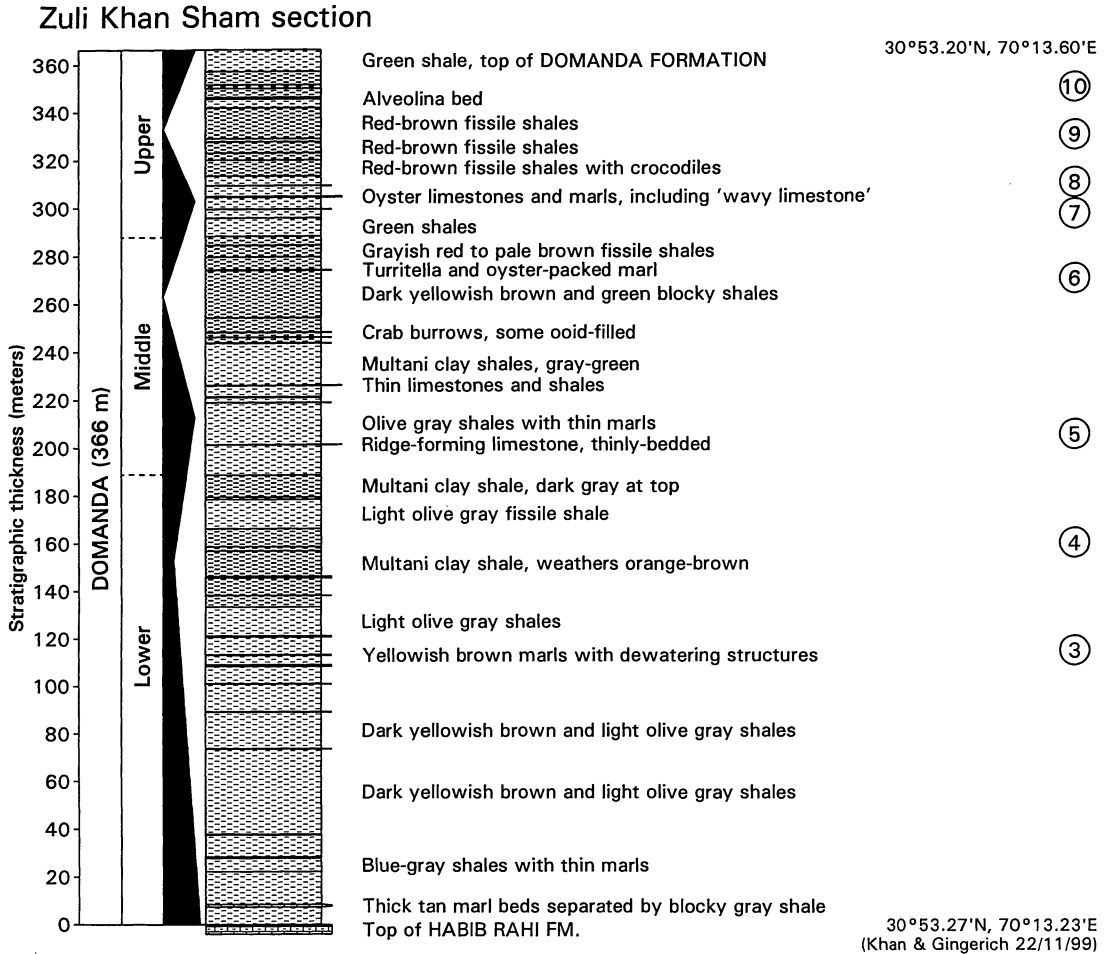


FIG. 5 — Zuli Khan Sham stratigraphic section of the 366 m thick Domanda Formation. Location of the Zuli Khan Sham traverse is shown on the map in Figure 2. Note the presence of three distinct cycles of limestones and/or green shales (lighter dashed fill pattern), changing upward to brown and red-brown shales (darker dashed fill pattern). These are interpreted as cycles of sea level flooding and shallowing, respectively. Sea level interpretation is shown by the width of the black band in the third column: this is widest during times of high sea stand and narrowest during times of low sea stand. Section log is recorded in Appendix table A-3. Circled numbers at right enumerate known archaeocete-bearing intervals within Lutetian strata of the Sulaiman Range (initiated in Fig. 3).

The interval from 188 to 244 m above the base of the Domanda Formation is again olive gray shales with thin limestones that indicate deeper water (Fig. 5; Appendix table A-3). The thin limestones are concentrated in two narrow intervals where they are ridge-forming, and there is a bivalve shell bed in between. The interval from 244 to 288 m is predominantly red and brown in color (Fig. 5; Appendix table A-3), indicating shallower water. Crab burrows and crab fossils are reasonably common, as are certain archaeocetes. Crocodiles are present but rare. The 288 m level in the Domanda Formation (Fig. 5) is taken as the top of the second shallowing-upward cycle of sea level change.

The interval from 288 to 314 m above the base of the Domanda Formation is predominantly composed of green shales, with two or sometimes three 15-30 cm-thick beds of oyster-rich, ridge-forming marl or impure limestone (Fig. 5; Appendix table A-3). These are clearly the "thin bands

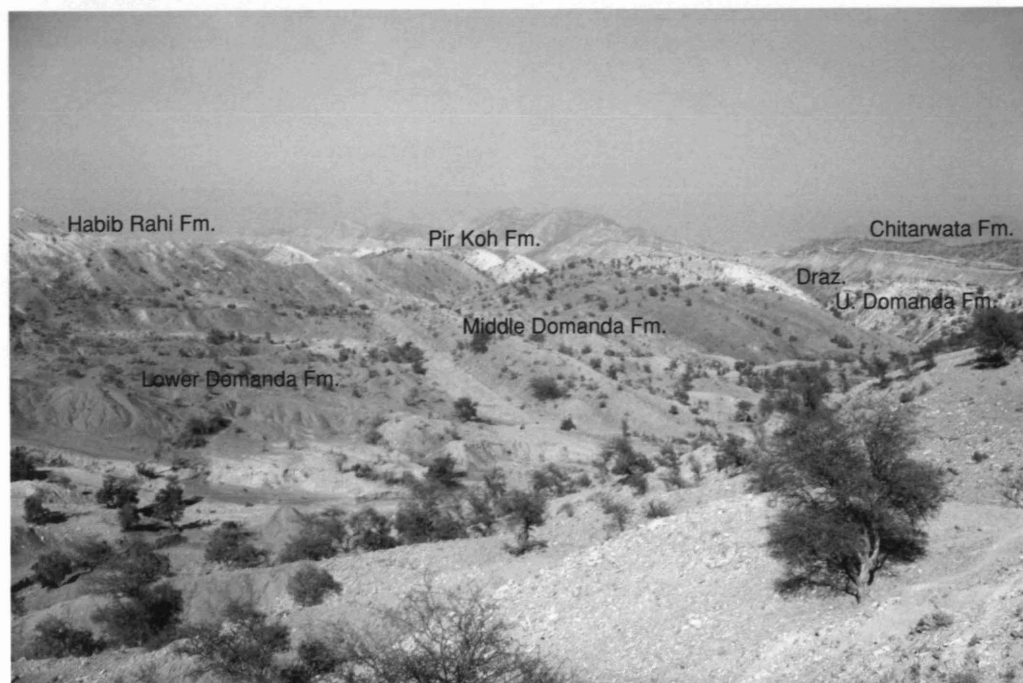


FIG. 6 — Photograph showing outcrop of Domanda Formation in the Zuli Khan Sham traverse just north of Zuli Khan Sham. View is to north. White band at left of photograph is Habib Rahi Formation. White band crossing right center of photograph is Pir Koh Formation. Ridge in distance at right side of photograph is upper Drazinda Formation capped by Chitarwata Formation sandstone. Note excellent exposure at all levels. Lower, middle, and upper Domanda labeled here represent three cycles of color change from light gray or green to darker brown and reddish brown. These correspond to divisions shown in the stratigraphic section of Fig. 5.

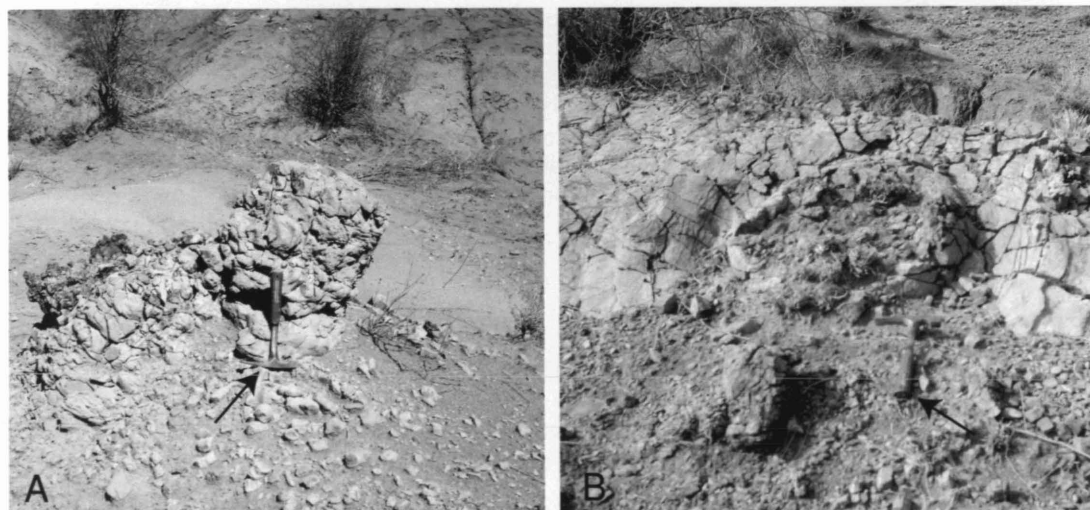


FIG. 7 — Marl or impure limestones found in the interval from 74 and 121 m above the base of the Domanda Formation (Fig. 5). A, vertical pillar of impure limestone penetrating light olive gray shales at about $30^{\circ} 59' N$, south of Baghobandkai; view is to northeast. B, flower-like circular structure in a yellowish brown marl at the 113 m level in the Zuli Khan Sham stratigraphic section (Fig. 5); structure is just north of the Zuli Khan Sham traverse at about $30^{\circ} 53.3' N$ and view is to west. Scale is given by hammer in each photograph (arrow).



FIG. 8 — Upper surface of 30 cm-thick 'wavy' limestone in the Domanda Formation 305 m above the base (Fig. 5). A, surface at about $30^{\circ} 51.75' N$ and $70^{\circ} 13.15' E$; view is to southwest. B, surface at about $30^{\circ} 51.20' N$ and $70^{\circ} 13.13' E$; view is to west. Note the presence of meter-scale undulations approximately parallel to strike, and decimeter-scale undulations approximately parallel to dip.

of impure limestone containing *Ostrea (Liostrea) pseudoflemingi* of Eames (1952a: 164), and certain archaeocetes are reasonably common in this interval. The middle limestone is generally the thickest and has a wavy upper surface (Fig. 8A,B) that the others lack. The interval from 314 m above the base to 366 m at the top of the Domanda Formation is predominantly composed of red-brown fissile shales (Fig. 5; Appendix table A-3). This interval has yielded distinctive archaeocetes and almost all of the crocodiles known from the Domanda Formation.

The age of the underlying Habib Rahi Formation is early Lutetian based on the presence of NP14-15 nannoplankton (Köthe et al., 1988; see below). Micropaleontological studies consistently describe the Domanda Formation as barren, however the overlying Pir Koh Formation has long been thought to be early Bartonian in age based on the presence of P12-13 planktonic Foraminifera (Samanta, 1973; see below). This indicates that the Domanda Formation is Lutetian in age and its great thickness means that it probably spans much of Lutetian time.

Sea level interpretation of the Habib Rahi and Domanda formations is relatively straightforward. The NP14-15 age of the Habib Rahi Formation means that it coincides with the major flooding event in the early Lutetian, which is consistent with a lithology of limestones containing thin bands of black chert. This grades upward into transitional gray and green shales and then brown shales representing a low sea stand. There are two additional cycles of high and then low sea stands in the Domanda Formation, with the high sea stands represented by green shales containing thin limestones and the low sea stands represented by brown and reddish brown shales. Intervals of flooding and shallowing are shown in the third column of Figure 5, where black predominates during intervals of sea level rise and flooding, and white predominates during intervals of sea level fall and shallowing. A Lutetian age for the combined Habib Rahi and Domanda formations in this and other sections is consistent with the general pattern of sea level change and with micropaleontological control where this is available (see below).

Baher Dabh Shumali section

The Pir Koh Formation and the Drazinda Formation are both represented in the Baher Dabh Shumali section (Fig. 9). The Pir Koh Formation is the "White Marl Band" of Eames (1952a). It is ridge-forming but commonly cross-cut by superimposed streams. In the Baher Dabh Shumali

section it has a total thickness of 19 m. This includes a 1.8 m thick, blocky, highly-burrowed marl at the base; a 5.7 m alternation of platy marls and blocky shales; a 4.8 m massive marl bed that weathers into laminae; and finally 7 m of gray shale and marl transitional to the lower Drazinda Formation (Fig. 9; Appendix table A-4).

The Drazinda Formation is equivalent to the vertical succession of "Passage Beds," "Upper Chocolate Clays," and "*Pellatispira* beds" described by Eames (1952a). It is in some ways similar to the Domanda Formation or "Lower Chocolate Clays" of Eames (1952a), but here five distinct cycles of flooding and shallowing are represented that are again evident in the pattern of color change observed in outcrop. The transition from the underlying Pir Koh Formation is gradational. Pir Koh marl bands thin upward and are separated by increasing thicknesses of gray-brown to blue-gray shale until the carbonate bands disappear. A photograph illustrating outcrop of the Drazinda Formation is shown in Figure 10.

The basal 92 m-thick interval of the Drazinda Formation (Appendix table A-5; 19-111 m interval in Fig. 9) is light-colored drab shales. These are overlain by 62 m of darker reddish brown shales with thin beds rich in mollusks and large 2-cm in diameter *Nummulites* (*N. beaumonti*; 111-173 m interval in Fig. 9). The upper part of these reddish brown shales is the interval that yielded *Babiacetus indicus* near Satta Post (Gingerich et al., 1995b). The first cycle of lower Drazinda flooding and shallowing begins with the Pir Koh flooding event at the base of the Baher Dabh Shumali section and ends at about the 173 m level (Fig. 9).

The interval from 173 m through 248 m in Figure 9 is predominantly composed of light olive gray to green clay shales (154 through 230 m interval in Appendix table A-5). There is a prominent, 70-cm thick, ridge-forming, *Discocyclusina sowerbyi*-packed marker bed 164 m above the base of the Drazinda section (183 m level in Fig. 9). The 40-m thick green shale, or here light olive gray shale, above the *Discocyclusina* marker bed is the stratigraphic interval that yielded numerous sea cows of the species *Protosiren sattaensis* (Gingerich et al., 1995b, 1997) and rare archaeocete whales of the basilosaurid species *Basilosaurus drazindai* and *Basiloterus hussaini* (Gingerich et al., 1997), again near Satta Post. The interval from 248 m through 303 m in Figure 9 is again darker maroon to reddish brown shales. This completes the middle Drazinda cycle of flooding and shallowing.

The upper part of the Drazinda Formation includes three thinner and presumably shorter cycles of flooding and shallowing, in the intervals from approximately 303 m through 360 m, 360 m through 391 m, and 391 m through 453 m, respectively, above the base of the Baher Dabh Shumali section shown in Figure 9 (Appendix table A-5).

The Pir Koh and Drazinda formations have yielded abundant microfossils, including planktonic forams and nannoplankton (Latif, 1964; Samanta, 1973; Köthe et al., 1988), and age control for the two formations is summarized below.

Sea level interpretation of the Pir Koh and Drazinda formations is again relatively straightforward, with lighter olive gray and green shales representing deeper water farther offshore, and darker reddish brown shales representing shallower water closer to the ancient shoreline. Intervals of flooding and shallowing are shown in the third column of Figure 9, where black predominates during intervals of sea level rise and flooding, and white predominates during intervals of sea level fall and shallowing.

The basal 6 m of the Chitarwata Formation overlying the Drazinda Formation is described in Appendix table A-5 to emphasize the lithological change from one to the other. Kirthar Group formations can be traced for hundreds of kilometers north and south along the eastern side of the Sulaiman Range, where there is virtually no clastic sediment coarser than silt (some siltstones and even sandstones are present farther to the north, and also farther to the west on the west side of the Sulaiman Range). The Chitarwata Formation, in contrast, starts with silty shale and siltstone at the base, and rapidly coarsens upward with a massive input of terrigenous clastic sediments indicating initiation of tectonic collision and mountain building on a locally unprecedented scale. Contact of the Drazinda and Chitarwata formations is conformable along much of the Sulaiman front, with no evidence of disconformity, raising a question of how much of a temporal gap, if any, may be represented between the two formations.

Baher Dabh Shumali section

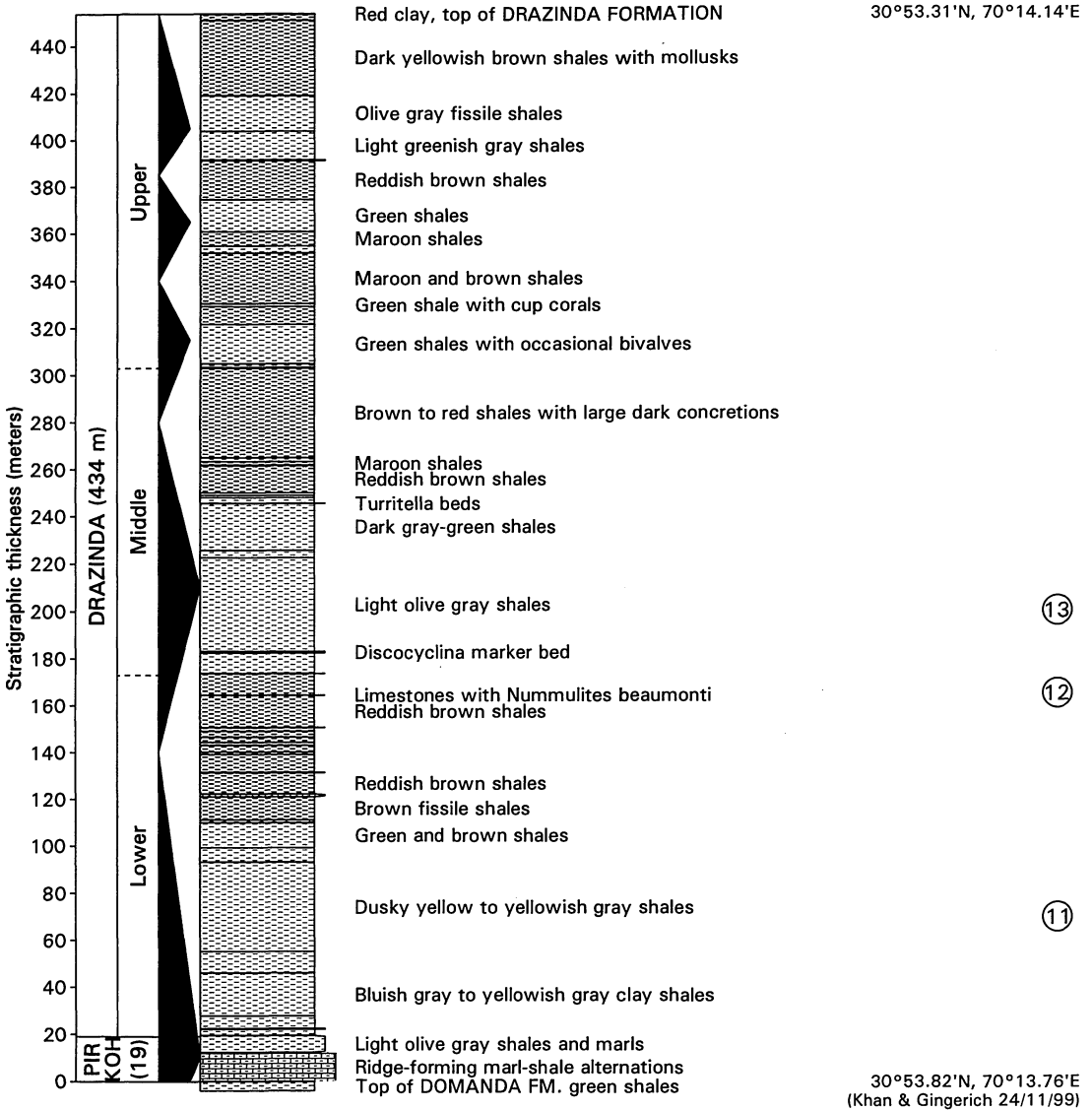


FIG. 9 — Baher Dabh Shumali stratigraphic section of the 19 m thick Pir Koh Formation and the 434 m thick Drazinda Formation. Location of the Baher Dabh Shumali traverse is shown on the map in Figure 2. Note the presence of five cycles of limestones and/or green shales (lighter dashed fill pattern) changing upward to brown and red-brown shales (darker dashed fill pattern). These are interpreted as cycles of sea level flooding and shallowing. Sea level interpretation is shown by the width of the black band in the third column: this is widest during times of high sea stand and narrowest during times of low sea stand. Section logs are recorded in Appendix tables A-4 and A-5. Circled numbers at right enumerate known archaeocete-bearing intervals within Bartonian strata of the Sulaiman Range (continuing the numbering sequence initiated in Figs. 3 and 5, and here based on limited prospecting).



FIG. 10 — Photograph of green and red shales of the Drazinda Formation exposed at the top of the Baher Dabh Shumali stratigraphic section. Photograph was taken standing on the Drazinda-Chitarwata contact, looking north along strike, with ridges of Pir Koh Formation and Drug Formation exposed in the background.

SUBDIVISIONS OF THE KIRTHAR GROUP AND THEIR CORRELATION AND AGE CALIBRATION

The middle and upper Eocene Kirthar Group comprising the Habib Rahi, Domanda, Pir Koh, and Drazinda formations together total 881 m of stratigraphic thickness in the Dabh area north of Drug Lahar. Three of the four formations have yielded numerous archaeocete whales, and the one that has not, the Pir Koh Formation, has not yet been searched systematically. The best age control for the four formations has been developed along strike at Rakhi Nala, 100 km south of the Dabh area, where relatively good sections are most easily accessible. Age control at Rakhi Nala is summarized in Figure 11.

It is clear from nannoplankton evidence that the Habib Rahi Formation is early Lutetian in age (NP14-15; Köthe et al., 1988). Planktonic foraminiferal evidence shows that the Pir Koh Formation is early Bartonian in age (P12-13; Samanta, 1973). And planktonic foraminiferal, nannoplankton, and shallow benthic foraminiferal evidence shows that the upper part of the Drazinda Formation is Priabonian in age (P15-17, NP18-20, and *Pellatispira*; Eames, 1952a; Samanta, 1973; Köthe et al., 1988). When the thicknesses of the Kirthar Group formations and their interpreted depths of deposition are evaluated subject to these constraints on age, there is a remarkable correspondence of sea level rise and fall documented locally to sea level rise and fall inferred globally (Fig. 11).

The Habib Rahi and Pir Koh carbonates are relatively deep-water tracts deposited during early Lutetian and initial Bartonian flooding. All three global Lutetian cycles of sea level rise and fall are observed in the Zuli Khan Sham section. Both Bartonian cycles and all three shorter Priabonian cycles are observed in the Baher Dabh Shumali section. It appears that the northwestern margin of

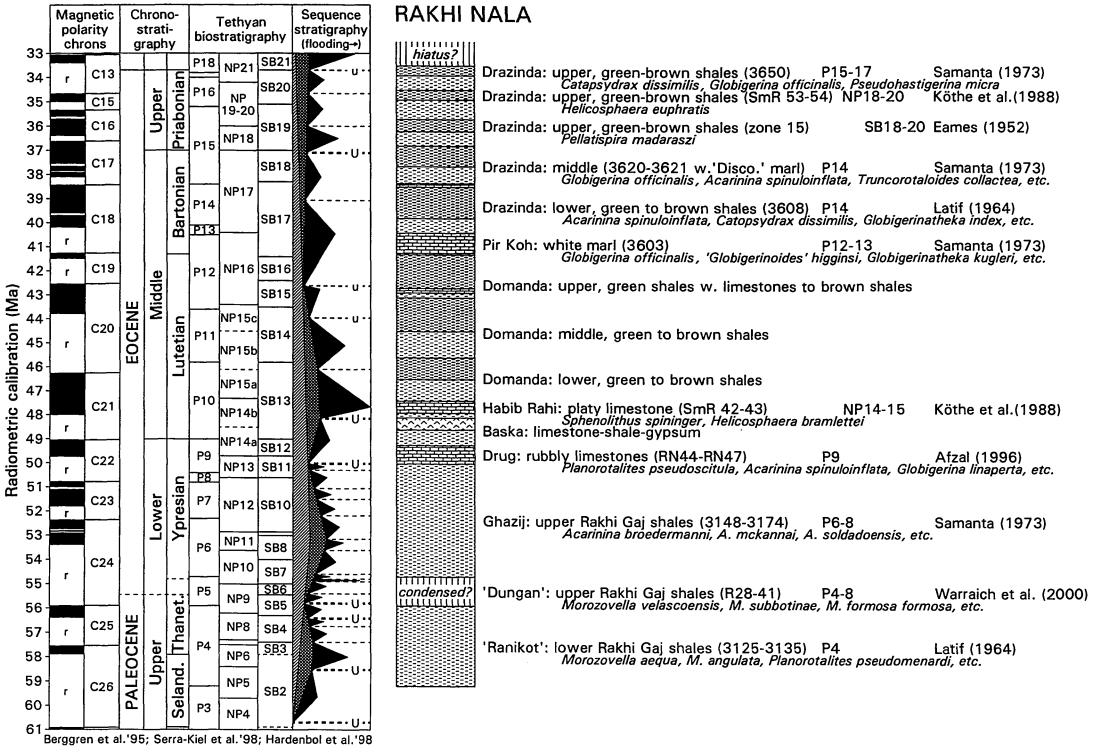


FIG. 11 — Temporal correlation chart for Paleocene-Eocene formations of Rakhi Nala 60 km along strike to the south of Dabh Nala, showing micropaleontological constraints on the age of the Drug, Habib Rahi, Pir Koh, and Drazinda Formations studied here. Left side of chart shows global magnetic polarity and chronostratigraphy, Tethyan biostratigraphy, and global sea level stratigraphy. Right side of chart shows lithology and associated planktonic foraminiferal (P), nannoplankton (NP), or shallow benthic (SB) ages, with literature references and lists of the more important index species. The time scale and planktonic zones shown here are from Berggren et al. (1995). Shallow benthic zones and correlation are from Serra-Kiel et al. (1998), and sea level stratigraphy is from Hardenbol et al. (1998).

the Indo-Pakistan subcontinent behaved passively enough during middle and late Eocene time to record a global pattern of sea level change without any substantial local tectonic overprint. The virtual absence of siltstones and coarser clastics along the Sulaiman front through the middle and late Eocene corroborates the requisite passivity of subsidence to record a global sea level signal.

Archaeocete whales are known from six stratigraphic intervals in the middle and upper parts of the Domanda Formation, which means that they probably span much of middle and late Lutetian time. Archaeocete whales described previously from the lower and middle Domanda Formation probably represent early and middle Lutetian time (Gingerich et al., 1993, 1994, 1995a). Sea cows and archaeocete whales described previously from the lower and middle Drazinda Formation probably represent middle Bartonian time (Gingerich et al., 1995b, 1997).

AGE OF THE WHALE-BEARING HARUDI FORMATION OF KUTCH

Some archaeocetes described here are similar to those known from the Harudi Formation of Kutch, in India, which were originally described as being Lutetian in age (e.g., Sahni and Mishra, 1972, 1975). This was at a time when the Lutetian stage or age was considered equivalent to all of

the middle part of the Eocene, and the Bartonian was considered more or less equivalent to the Priabonian in the upper or late Eocene (e.g., Berggren, 1972). However, development of global correlation based on planktonic foraminiferan (P) and nannoplankton (NP) zones showed that the type Bartonian is P13-14 and NP17 in age, and it was moved to the middle Eocene (Hardenbol and Berggren, 1978). Later time scales used for global correlation follow this convention (e.g., Harland et al., 1982, 1990; Berggren et al., 1995). Bajpai and Thewissen (1998, 2000) and Williams (1998) continued to use the term Lutetian as if it is a equivalent to the whole middle Eocene, which is confusing and anachronistic.

The standard reference on Kutch stratigraphy is Biswas (1992), who cited Mohan and Soodan (1970) for planktonic foraminiferal zonation, and Singh and Singh (1991) for nannoplankton zonation of the Harudi and overlying Fulra formations. Mohan and Soodan's results (1970, p. 39) can be grouped into nine stratigraphically-superposed sets of samples of temporally informative planktonic forams. These are analyzed in Figure 12. Mohan and Soodan (1970, p. 40) described the record of planktonic Foraminifera in the two lower sets of samples (1345-1333) as "poor, perhaps due to an unsuitable environment and the frequent variations in depositional conditions." Samples in sets 3 through 9 are richer and generally have a larger number of temporally-informative species. All of these yield ages of P12-13 and are consistent with an early Bartonian age. Singh and Singh (1991) and Jafar and Rai (1994) found nannoplankton from the Harudi and Fulra formations of Kutch to represent zones NP16-17, corroborating the early Bartonian age based on planktonic forams.

Results for Kutch can be plotted on a temporal correlation chart (Fig. 13) like that constructed for Rakhi Nala. Aligning the Harudi and Fulra formations with the early Bartonian flooding event satisfies temporal constraints on the age of these formations and reflects the view that Kutch was an eroding land surface during much of Eocene time, being flooded in the early Eocene when the Naredi Formation was deposited and again in Bartonian middle Eocene time when the Harudi and Fulra formations were deposited (e.g., Singh and Singh, 1991, p. 30). There is also some evidence of a later flooding event in the Priabonian (Biswas, 1992). An early Bartonian age for the Kutch formations yielding archaeocetes means that these together represent a relatively short interval of Eocene time, and that this corresponds temporally to deposition of the Pir Koh Formation in Pakistan, providing information about the archaeocete fauna for an interval that remains to be investigated in the Sulaiman Range. The entire Harudi Formation is on the order of 14 m thick (Biswas, 1992), which is about 1.6 percent of the 881 m thickness of Kirthar formations under study here.

SYSTEMATIC PALEONTOLOGY

Class MAMMALIA Linnaeus, 1758

Order CETACEA Brisson, 1762

Suborder ARCHAEOCETI Flower, 1883

Family REMINGTONOCETIDAE Kumar and Sahni, 1986

Type genus.— *Remingtonocetus* Kumar and Sahni, 1986, p. 330.

Included genera.— *Andrewsiphius* Sahni and Mishra, 1975, p. 23; *Remingtonocetus* Kumar and Sahni, 1986, p. 330; *Dalanistes* Gingerich, Arif, and Clyde, 1995a, p. 317; *Attockicetus* Thewissen and Hussain, 2000, p. 135.

Diagnosis.— Remingtonocetidae differ from all other archaeocetes in having long, narrow skulls; external nares opening well forward on the skull; frontal shield narrow; orbits small; full complement of upper and lower teeth (dental formula 3.1.4.3 / 3.1.4.3); palate convex; and mandibular symphysis unfused. Postcranially, remingtonocetids have relatively long cervical vertebrae; sacrum composed of four vertebrae, with at least the anterior three solidly fused; acetabular notch in pelvis narrow to closed; femoral head lacking a distinct fovea.

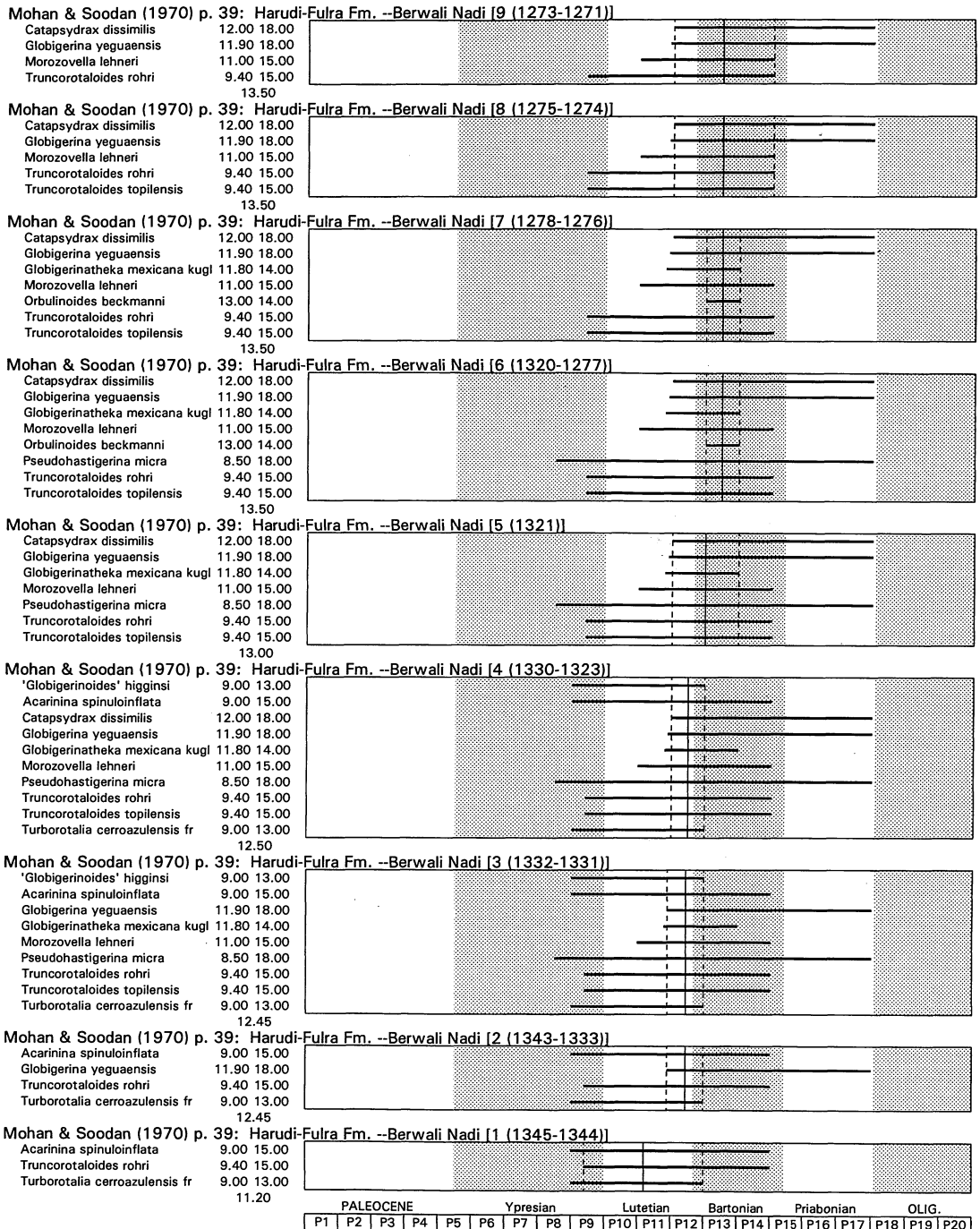


FIG. 12 — Planktonic foraminiferal age control for the middle Eocene Harudi and Fulra formations in the Berwali Nadi area of Kutch in Gujarat, India. Age ranges of temporally-informative planktonic forams reported by Mohan and Soodan (1970) are shown on the planktonic foraminiferal time scale of Toumarkine and Luterbacher (1985). Solid vertical line marks the median of first and last appearances of all lineages (the median of the zone numbers tabulated to the left of each range chart), and dashed vertical lines mark ends of ranges closest to median to show intervals of consistency. Median shows slight trend toward

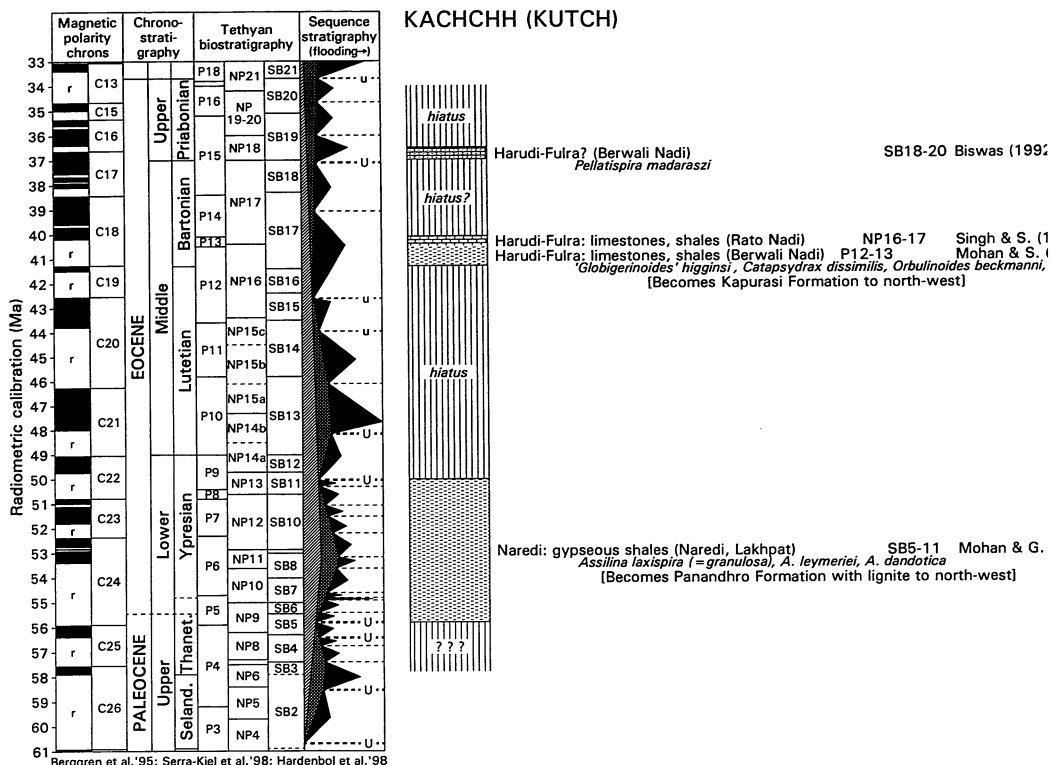


FIG. 13 — Temporal correlation chart for Eocene formations of Kutch (Gujarat, India), showing micropaleontological constraints on the age of the Naredi Formation and on the age of the Harudi and Fulra formations of interest here. Left side of chart shows global magnetic polarity and chronostratigraphy, Tethyan biostratigraphy, and global sea level stratigraphy. Right side of chart shows lithology and associated planktonic foraminiferal (P), nannoplankton (NP), or shallow benthic (SB) ages, with literature references and lists of the more important index species. The time scale and planktonic zones shown here are from Berggren et al. (1995). Shallow benthic zones and correlation are from Serra-Kiel et al. (1998), and sea level stratigraphy is from Hardenbol et al. (1998).

Discussion.— Anterior teeth of *Remingtonocetus* described below are mediolaterally flattened somewhat like those of the mako shark *Isurus*. If typical of the family, this is an important distinction from contemporary Protocetidae, which have more conical anterior teeth. Shark-like anterior teeth may provide a clue to the feeding strategy of remingtonocetid whales, which are also distinctive in having relatively long necks and long, narrow skulls.

Andrewsiphius Sahni and Mishra, 1975

Type species.— *Andrewsiphius kutchensis* Sahni and Mishra, 1975, p. 23.

Included species.— *Protocetus sloani* Sahni and Mishra, 1972 [= *Andrewsiphius kutchensis* Sahni and Mishra, 1975].

younger age at top of section, as expected. All samples are consistent with an early Bartonian P12-13 age. Ypresian and Bartonian marine stages/ages and the Oligocene epoch with stippling are distinguished from the Paleocene, intervening Lutetian, and Priabonian without stippling.

Diagnosis.— *Andrewsiphius* differs from *Remingtonocetus* and *Dalanistes* in being smaller, having a narrower rostrum, and in having smaller premolars that are separated by relatively longer diastemata.

Discussion.— The type specimen of the type species of *Andrewsiphius*, *Andrewsiphius kutchensis* Sahni and Mishra (1975, p. 23; LUVF 11060), and the type specimen of the referred species *Andrewsiphius minor* Sahni and Mishra (1975, p. 25; LUVF 11165) were described as mandibular fragments, and this interpretation persists (e.g., Williams, 1998, p. 8), but each appears to be maxillary. Unusual characteristics attributed to *Andrewsiphius*, such as confluence of the mandibular canals anteriorly (these are nasal passages), and extension of the mandibular symphysis posteriorly as far as M₃ (this is the palate) make sense if the ‘mandibular’ fragments are in fact maxillary. Complicating matters, most types and other described specimens of *Andrewsiphius* are gypsified and have not been prepared adequately for study.

The type specimen of *Protocetus sloani* Sahni and Mishra (1972), later *Remingtonocetus sloani* (Kumar and Sahni, 1986), was described as a mandibular fragment (Sahni and Mishra, 1972, p. 492; 1975, p. 25; Kumar and Sahni, 1986, p. 341; Williams, 1998, p. 8; LUVF 11002), but it too is maxillary and compares closely to *Andrewsiphius* rather than *Remingtonocetus*. A referred specimen of *Remingtonocetus harudiensis* (Kumar and Sahni, 1986, p. 336; LUVF 11132) is undoubtedly maxillary and compares closely with *Andrewsiphius* rather than *Remingtonocetus*.

All of these specimens are within the normal range of variation in size for a species, and here we recognize a single species of *Andrewsiphius*, *Andrewsiphius sloani* (Sahni and Mishra, 1972), from the early Bartonian Harudi Formation of Kutch. We regard the similar-sized *Andrewsiphius kutchensis* Sahni and Mishra (1975), *Andrewsiphius minor* Sahni and Mishra (1975), and *Kutchicetus minimus* Bajpai and Thewissen (2000) as junior synonyms of *A. sloani*. Recognition of any of these species as distinct will require comparison with previously described types and more justification than has been published to date.

The type specimen of *Andrewsiphius sloani* came from the Chocolate Limestone of Harudi (Kumar and Sahni, 1986, p. 341), as did the type of *Kutchicetus minimus*. Bajpai and Thewissen (2000, p. 1478) wrote that *Kutchicetus minimus* “can be diagnosed from other remingtonocetids on the basis of its small size,” and claimed that it is “less than half the size (in linear dimensions) of the smallest known remingtonocetid (*A. minor*)” without presenting any quantitative comparison that might provide a basis or explain the rationale for this claim. Lumbar centrum lengths of 38–40 mm for *Kutchicetus minimus* (plotted in Bajpai and Thewissen’s fig. 4) are only about 20–25 percent smaller than comparable dimensions of medium-sized *Remingtonocetus* cf. *R. harudiensis* (listed in table 5 of Gingerich et al., 1995a), which is about the difference to be expected for *Andrewsiphius sloani*.

Andrewsiphius sloani (Sahni and Mishra, 1972)

Fig. 14

Holotype.—LUVF 11002, maxillary fragment with alveoli for double-rooted P³, P⁴, and M¹.

Type locality.— Chocolate limestone 3 km southeast of Baranda or 2 km northwest of Harudi in southwestern Kutch, India (Sahni and Mishra, 1972; Kumar and Sahni, 1986).

Diagnosis.— As for the genus.

Age and distribution.— *Andrewsiphius sloani* is known from the upper Domanda Formation (late Lutetian) of Pakistan and from the Harudi Formation (early Bartonian) of India.

Newly referred specimens.— GSP-UM 3307, three pieces of a skull, including a well preserved piece of maxillary rostrum, from green shales just above the wavy limestone in the lower part of the upper Domanda Formation, at 30° 51.79' N latitude, 70° 13.25' E longitude. GSP-UM 3393, partial braincase with natural endocast, from reddish brown shales in the middle of the upper Domanda Formation, at 30° 53.50' N latitude, 70° 13.60' E longitude. The first locality is in Ander Dabh Janubi and the second is in Ander Dabh Shumali, both near Drug, in easternmost Baluchistan Province, Pakistan.

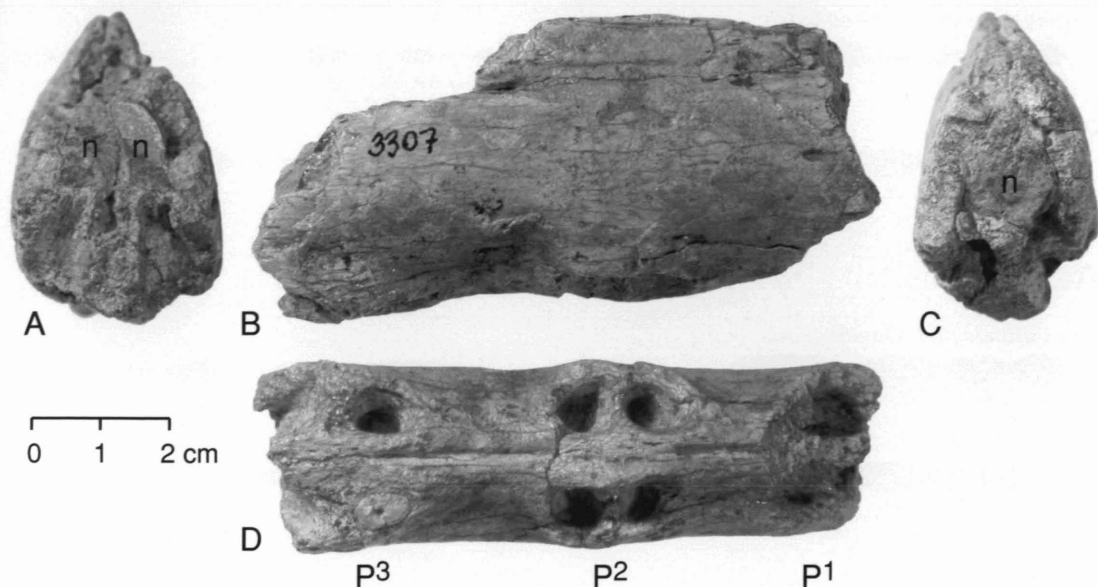


FIG. 14 — New specimen of *Andrewsiphius sloani*, GSP-UM 3307, piece of maxillary rostrum, in posterior (A), right lateral (B), anterior (C), and occlusal views (D). Abbreviation: *n*, narial passage (divided in posterior view). Scale is in cm.

Description.— The most informative new specimen of *Andrewsiphius sloani* is the partial maxillary rostrum of the type, GSP-UM 3307 (Fig. 14A-D). Left and right maxillae and left and right nasals are all fully co-ossified with no trace of sutures between them, indicating that the individual was fully adult. The rostrum is 90 mm in length as preserved, 25.2 mm wide at the position of P¹, 27.4 mm wide at the position of P², and 28.0 mm wide at the position of P³. It is, in contrast, 43.0 mm high at the position of P², giving it the narrow and high cross section typical of remingtonocetids. The narial passage through the rostral piece is well preserved. This is undivided in front where it is exposed above the alveoli for left and right P¹, but divided by a bony septum in back above the alveoli for left and right P³. This demonstrates that the rostral piece is in fact rostral and not fused left and right dentaries. Alveoli for single-rooted P¹ measure 9.7 mm anteroposteriorly and 6.0 mm mediolaterally. These are followed by a diastema of about 19 mm. Alveoli for double-rooted P² measure 18.0 mm in anteroposterior length and about 6.8 mm in mediolateral breadth. These are followed by a diastema of 20 mm. Alveoli for double-rooted P³ measure approximately 21.5 mm in anteroposterior length and about 7.3 mm in maximum mediolateral breadth. We have not yet been able to identify the accompanying two cranial fragments as to position in the cranium.

A second new specimen is GSP-UM 3393, a partial braincase with much of a natural endocast. This is small and measures approximately 58 mm in breadth between left and right internal auditory meati.

Remingtonocetus Kumar and Sahni, 1986

Type species.— *Protocetus harudiensis* Sahni and Mishra, 1975, p. 21.

Included species.— *Remingtonocetus harudiensis* (Sahni and Mishra, 1975), and *Remingtonocetus domandaensis* new species.

Diagnosis.— *Remingtonocetus* differs from *Andrewsiphius* in being larger, with a broader rostrum and longer premolars. Differs from *Dalanistes* in being smaller, with more gracile premolars and molars; P₄ and M₁ are larger relative to other teeth, while M₂ and M₃ are smaller both absolutely and relatively in *Remingtonocetus* (Fig. 15).

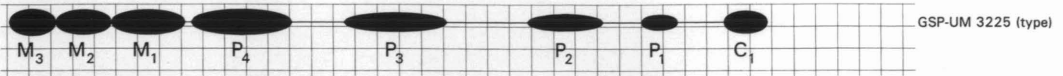
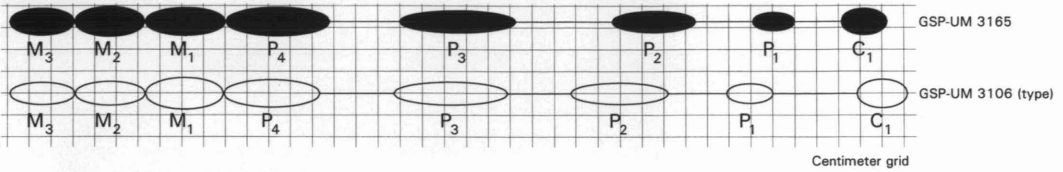
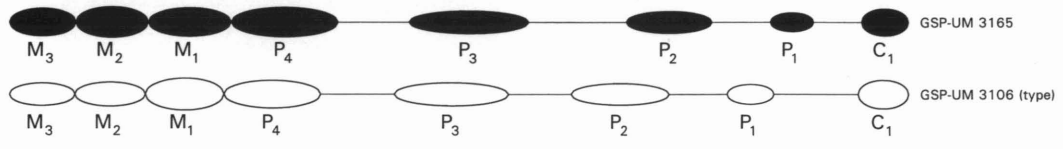
Remingtonocetus domandaensis*Dalanistes ahmedi**Remingtonocetus domandaensis**Dalanistes ahmedi*

FIG. 15 — Absolute and proportional differences in lower cheek teeth of *Remingtonocetus domandaensis* and *Dalanistes ahmedi*. Major axis of ellipse representing each tooth is crown length (closed ellipses) or alveolus length (open ellipses), minor axis of ellipse is crown or alveolus width, and separation between ellipses is diastema length. A, comparison of absolute sizes and separation of C₁-M₃ in holotype of *Remingtonocetus domandaensis* (GSP-UM 3225) with those in holotype (GSP-UM 3106) and referred specimen (GSP-UM 3165) of *Dalanistes ahmedi*. Specimens are drawn to the same scale (grid squares are one centimeter on a side). B, comparison of relative sizes and separation of C₁-M₃ in holotype of *Remingtonocetus domandaensis* (GSP-UM 3225) with those in holotype (GSP-UM 3106) and referred specimen (GSP-UM 3165) of *Dalanistes ahmedi*. Specimens are drawn to the same C₁-M₃ length. Specimens shown here are all from the upper part of the middle Domanda Formation (middle Lutetian). Note the smaller absolute size of the dentition in *Remingtonocetus domandaensis*, and the relatively larger P₄-M₁ and smaller M₂-M₃ in this species.

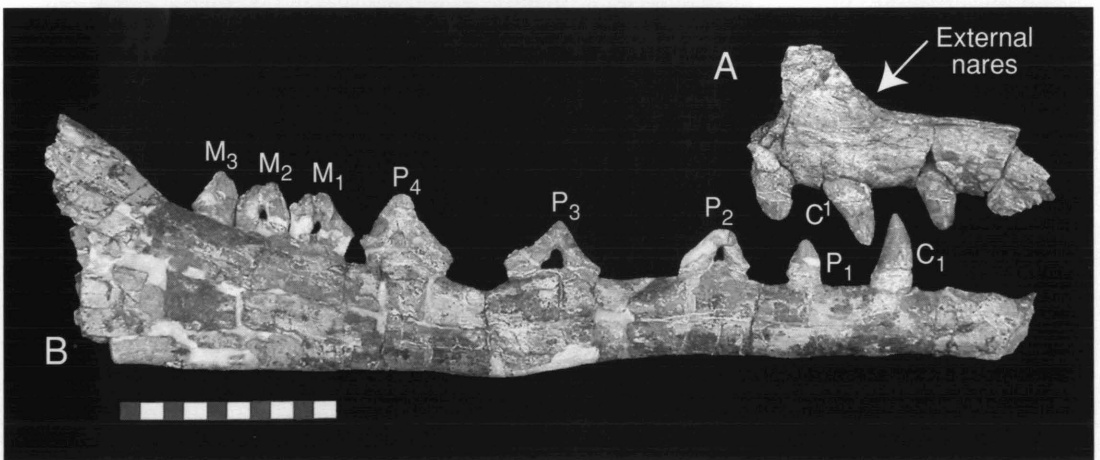


FIG. 16 — Dentition of *Remingtonocetus harudiensis*, new species, GSP-UM 3325 (holotype). A, rostrum in right lateral view, with alveolus for I¹, root of I², and intact crowns of I³, C¹, and P¹. Note external nares opening directly above C¹. B, right dentary in right lateral view, with alveolus for I₃ and intact crowns of C₁-M₃. Scale is in cm.

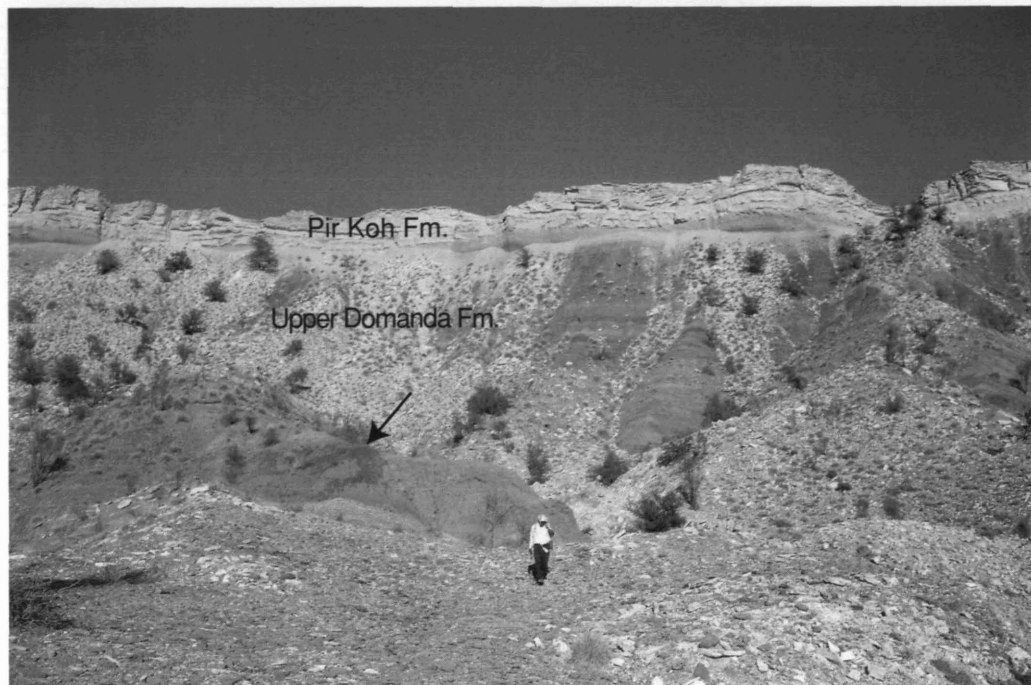


FIG. 17 — Type locality of *Remingtonocetus harudiensis*, new species. Locality of GSP-UM 3325 (holotype; arrow) is in the upper part of the middle Domanda Formation at Ander Dabh Shumali at $30^{\circ} 59.14' N$ latitude and $70^{\circ} 13.18' E$ longitude. View is to the east. Section in background includes lower and upper parts of the upper Domanda Formation capped by the ridge-forming Pir Koh Formation.

***Remingtonocetus domandaensis* new species**

Fig. 16

Holotype.— GSP-UM 3225, partial cranium and right dentary with C_1 - M_3 of a fully adult individual. Associated postcranial elements include five cervical vertebrae, three thoracics, two lumbar, one caudal, and numerous ribs.

Type locality.— Ander Dabh Shumali at $30^{\circ} 59.14' N$ latitude, $70^{\circ} 13.18' E$ longitude (Fig. 17), near Drug in easternmost Baluchistan Province, Pakistan. Type specimen was recovered from reddish brown shales in the upper part of the middle Domanda Formation. This is middle Lutetian in age.

Diagnosis.— Similar to *Remingtonocetus harudiensis* but differs in details of molar morphology. M_1 and M_2 have second apical cusps following the first, which are not seen in LUVF 11037, the holotype of *R. harudiensis*. M_2 is notably more massive. Its anterior crest in front of the apical cusp, and especially the posterior crest behind the apical cusp are expanded and convex upward, while they are straight and concave, respectively, in the type of *R. harudiensis*.

Age and distribution.— *Remingtonocetus domandaensis* ranges from the upper part of the lower through the upper part of the upper Domanda Formation throughout the Sulaiman Range of Pakistan. The species ranges from early through late Lutetian in age.

Hypodigm.— GSP-UM 3009, 3015, 3052, 3054, 3057, 3101 described previously (Gingerich et al., 1993, 1995a). GSP-UM 3225 (holotype), listed above; GSP-UM 3408, partial skeleton with vertebrae including sacrum, innominates; GSP-UM 3415, well preserved cranium with all alveoli and intact crowns of P^3 and M^{1-3} .

TABLE 2 — Measurements of teeth in the type specimen of *Remingtonocetus domandaensis* GSP-UM 3225. Measurements in parentheses are based on alveoli. All measurements are in mm. Asterisks denote estimates.

Tooth position	Crown length	Crown width	Apical height	Trailing diastema
<i>Upper dentition</i>				
I ¹	—	—	—	8.5
I ²	22.3	11.6	—	17.4
I ³	17.1	10.0	19.5*	26.0
C ¹	20.0	9.9	24.4*	11.5
P ¹	20.0	6.8	13.0*	—
<i>Lower dentition</i>				
I ₃	(19.5)	(10.0)	—	17.0
C ₁	19.8	9.9	28.5	21.5
P ₁	16.6	6.7	17.2	17.5
P ₂	34.2	7.4	19.5	36.8
P ₃	46.5	8.4	23.0	24.0
P ₄	46.3	11.3	27.0	3.0
M ₁	33.8	11.0	18.0	—
M ₂	25.7	11.0	19.6	—
M ₃	21.2	11.8	19.4	—

Etymology.— Named for the Domanda Formation yielding the type and all known specimens.

Description.— GSP 3225 (holotype) comprises parts of a cranium, including the well preserved anterior part of the rostrum with crowns of I²⁻³, C¹, and P¹. The premaxillae in this rostrum piece are solidly fused to the maxillae, with no remaining suture, which taken together with other evidence indicates the specimen was fully mature. This rostral piece shows the external nares to have opened anteriorly at a point directly above the upper canines (Fig. 16A). I¹ is represented on the right side of the rostrum by a large alveolus, and I² is represented by its root. I¹ and I² appear to have been about the same size. The crowns of the right I³, C¹, and P¹ were found separately during excavation but these fit into the remaining alveoli in the rostrum. I¹ through P¹ are all single-rooted. The root of I³ is smaller than those of I¹ and I². The crown of I³ is unusual in being straight and symmetrically flattened mediolaterally. The crown of C¹ is mediolaterally flattened but more curved, with the anterior margin of the tooth being convex anteriorly and the posterior margin concave posteriorly, while the labial surface is convex laterally and the lingual surface is concave medially. The crown of P¹ is similar to those in front of it, but low and blunt. Crowns of I³-P¹ all bear faint labial and lingual cingula surrounding the base of the crown. Measurements of these upper teeth are listed in Table 2.

The cranium of GSP 3225 also includes the posterior part of the braincase with large and posteriorly-projecting nuchal crests. The right exoccipital is well preserved, projecting laterally some 12.5 cm from the midline of the skull. Thus the width across the exoccipitals was about 25.0 cm, two cm greater than that reported for GSP-UM 3052 (first identified as *Dalanistes* in Gingerich et al., 1995a, but here referred to *Remingtonocetus*). The referred skull, GSP-UM 3408, has a condylobasal length of 75 cm.

The right dentary of GSP 3225 is broken through the alveolus for I₂ and behind M₃. The rest is well preserved (Fig. 16B). The mandibular symphysis extends posteriorly to a point beneath P₃, and the posterior part of the dentary is hollow, reflecting the presence of a much enlarged mandibular canal associated with hearing in cetaceans. All of the lower cheek teeth have narrow and delicate crowns with the exception of P₄-M₃, which are a little more robust.

The lower canine, C₁, is single-rooted, and the crown is relatively high and straight. It is narrow, with a slightly convex anterior margin and a slightly concave posterior margin. Very weak labial and lingual cingula encircle the crown. P₁ is single-rooted with a simple, narrow, relatively low, triangular crown. Again this is encircled by faint labial and lingual cingula. P₂ is double-

rooted like all following teeth. It has a uniformly low crown arched in a distinctive way to make the apex much higher than the height at the front or back of the crown (apex height rather than crown height is reflected in ordinary measurements). The anterior crest of the tooth is straight and rises steeply in front of the apical cusp, while the posterior crest is concave upward and rises less steeply. The crown of P_3 is similar to that of P_2 , but both crests, anterior and posterior to the apex, are serrated, and both are flexed, rising more steeply in the middle. The posterior part of the crown of P_3 has serrations enlarged into several distinct cusps. The crown of P_4 is higher and more substantial than that of either P_2 or P_3 . It mirrors P_2 and P_3 to some extent in having cusps on the crest anterior to the apical cusp. This crest is long, slightly concave upward, and rises less steeply than the crest posterior to the apical cusp. The posterior crest is serrated, straight, and steeply angled.

M_1 is distinctive in having a long, sloping, concave-upward crest in front of its apical cusp. There are two accessory cusps, the first one large, behind the apical cusp. M_2 is the most massive of the molars. Crests in front of and behind the apical cusp are convex upward. M_2 has a second large cusp behind the apical cusp, and three smaller cusps behind that. M_3 has an unusual shape in that there is a short crest, sloping slightly, anterior to the apical cusp, and a steeply-sloping rounded surface descending behind the apical cusp. M_1 is the longest of the molars, and the shortest is clearly M_3 . The proportions of the lower cheek teeth are illustrated in Figure 15, and measurements of all teeth are listed in Table 2. Five additional tooth crowns of uncertain position were found with the type when it was excavated.

Postcranial elements associated as part of the holotype include a well preserved atlas. This is large, measuring 18.5 cm in maximum breadth, and it is distinctively flexed both ventrally in the sagittal plane and backward in the coronal plane. The ventral flexion indicates notable angulation between the long axis of the skull and the neck in life. Centra of the axis and cervicals C3, C6, and C7 are long, with articular surfaces angled as described previously (Gingerich et al., 1995a, p. 315). C6 has its ventrally-deflected transverse processes intact. These are massive and descend some 8 cm below the base of the centrum. C7 is virtually complete. Remaining vertebrae will be described when they are studied in the context of other known *Remingtonocetus* skeletons. Ribs are gracile and almost circular in cross-section.

The sacrum is well preserved in GSP-UM 3408. This is a four-centrum sacrum very similar to that of *Dalanistes ahmedi* described previously, but it is smaller, measuring 20 cm in length rather than the 23-25 cm reported for *Dalanistes* by Gingerich et al. (1995a, p. 326). Innominates of GSP-UM 3408 are distinctive in having an acetabulum with a lunate surface that is not lunate in shape but rather encircles a foramen-like acetabular fossa completely. There is no acetabular notch, per se, but rather an acetabular canal, covered by the expanded lunate surface, communicating with the acetabular fossa and supplying nutrients to the articular capsule. The ilium is long and high, providing a large surface for origination of gluteal musculature.

Discussion.— *Remingtonocetus domandaensis*, with a condylobasal skull length of 75 cm, is virtually identical in size to *Remingtonocetus harudiensis*, for which Kumar and Sahni (1986, p. 331) report a skull length of 75 cm. The type specimen of *Dalanistes ahmedi*, in contrast, has a condylobasal length estimated at 90 cm (Gingerich et al., 1995a, p. 320). Thus *R. domandaensis* is about 17 percent smaller in this dimension than contemporary *D. ahmedi*. This difference shows up too in Figure 15, where the ratio of C_1 through M_3 length in *R. domandaensis* to those in *D. ahmedi* are $347/410 = 0.85$ and $347/401 = 0.87$, respectively. Taken together, these measurements mean *R. domandaensis* is 17-13 percent, averaging 15 percent, smaller than contemporary *D. ahmedi*. *Remingtonocetus* and *Dalanistes* also differ in the proportions of their lower premolars and molars (Fig. 15).

It is difficult to compare *Remingtonocetus domandaensis* in detail to *R. harudiensis*. The type of the latter, LUVF 11037, is a fragmentary skull with roots for P^4 - M^3 , left and right mandibular rami with roots for P_4 - M_3 , much of the crown of an upper molar, isolated cusps of upper teeth, and crowns of left M_1 and M_2 (Sahni and Mishra, 1975, p. 21). This came from the Chocolate Limestone of the Harudi Formation 2 km north of Harudi, in southwestern Kutch, Gujarat, India ($23^\circ 30.33'$ N latitude, $68^\circ 41.25'$ E longitude). The lower molars, M_1 and M_2 , were described and

illustrated by Sahni and Mishra (1975, pl. 4: 6), Sahni (1981, pl. 1: 1), and Kumar and Sahni (1986, fig. 8e-h). These are relatively gracile, and bicuspid in the sense that they have a single high apical trigonid cusp and a lower talonid cusp. The crest anterior to the apical cusp is virtually straight, while the posterior crest is concave upward. M_1 and M_2 in GSP-UM 3225 have second apical cusps following the first, which are not seen in LUVP 11037. In addition, M_2 is notably more massive, and the anterior crest and especially the posterior crest are expanded and convex upward.

LUVP 11132, described by Kumar and Sahni (1986, p. 331, fig. 10g-j) as the anterior portion of a mandible referred to *Remingtonocetus harudiensis*, is neither the anterior portion of a mandible nor *Remingtonocetus*, but rather the rostrum of a skull of *Andrewsiphius* (see above).

Remingtonocetus domandaensis is interpreted as a similar-sized but older and more generalized member of the evolutionary lineage leading to *R. harudiensis*. Closure of the acetabular notch in the pelvis is consistent with a smooth to shallowly developed fovea capitis femoris on the femur, noted previously (Gingerich et al., 1997, p. 315), suggesting that the round ligament anchoring the femoral head in the acetabulum was insubstantial if present at all. This might indicate in turn that the hind limb of *Remingtonocetus* was not weight-bearing in the ordinary sense. The femur is relatively short and robust, with a high greater trochanter and a laterally-expanded diaphysis suggesting the presence of powerful hip extensors and femoral adductor musculature. When considered together with the presence of shark-like anterior teeth, one gains an impression that *Remingtonocetus* may have been a specialized and efficient swimmer. The solidly fused sacrum might have limited tail-powered locomotion but at the same time provided a strong base for foot-powered swimming. Recovery and study of increasingly better postcranial remains should clarify the locomotor and other aquatic specializations of *Remingtonocetus*.

Dalanistes Gingerich, Arif, and Clyde, 1995

Type species.— *Dalanistes ahmedi* Gingerich, Arif, and Clyde, 1995, p. 317.

Included species.— Type species only.

Diagnosis.— Differs from *Andrewsiphius* in being larger, with a broader rostrum and longer premolars. Differs from *Remingtonocetus* in being larger, with more robust premolars and molars; P_4 and M_1 are smaller relative to other teeth, and M_2 and M_3 are larger both absolutely and relatively (Fig. 15).

Discussion.— As more has been learned about *Remingtonocetus*, it has become clear that *Dalanistes* is more similar in overall proportions and morphology to *Remingtonocetus* than was evident when *Dalanistes* was named, raising the possibility that these could be congeneric, or even males and females of the same genus and species. However, differences in cheek tooth proportions shown in Fig. 15 would not be expected in different species of a genus, and these differences in proportions, plus the observed absolute differences in molar size, would not be expected in a dimorphic species. Pending recovery of larger samples, we regard *Dalanistes* and *Remingtonocetus* as two similar and closely related remingtonocetid genera.

Dalanistes ahmedi Gingerich, Arif, and Clyde, 1995

Holotype.— GSP-UM 3106, partially articulated skull and postcranial skeleton.

Type locality.— Basti Ahmed, in Dalana Nala drainage in saddle just to the south of Takra valley, 30° 07.55' N latitude, 70° 21.92' E longitude.

Diagnosis.— As for the genus.

New specimens.— GSP-UM 3295, immature skull with crowns or alveoli for all deciduous cheek teeth, crowns of M^{1-2} fully erupted, and crowns of M^3 just beginning to erupt on both sides of the palate.

Description.— Specimen will be described elsewhere as part of a larger study of *Dalanistes*.

Discussion.— GSP-UM 1856, a partial cranium described by Gingerich et al. (1995a, p. 311),

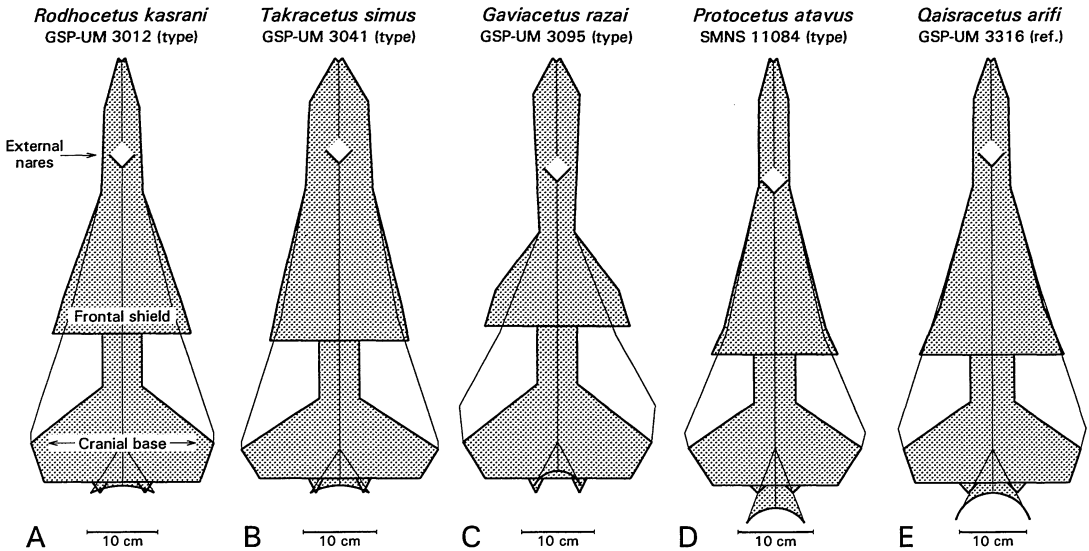


FIG. 18 — Diversity of cranial morphology in early Protocetidae, ordered from oldest (left) to youngest (right). Cranium of *Rodhocetus kasrani* (A; early middle Lutetian) is compared to those of *Takracetus simus* (B; early middle Lutetian), *Gaviacetus razai* (C; middle Lutetian), *Protocetus atavus* (D; middle Lutetian), and *Qaisracetus arifi* (E; late Lutetian). Schematic drawings, in dorsal view, are scaled to same condylobasal length (original skulls are close to the same size). *Qaisracetus* is a relatively generalized protocetid, but the anterior position of the external nares, relatively large orbits, and the large nuchal crest visible here are some of the characteristics that distinguish *Qaisracetus* from other genera. Differences in rostral shape shown here reflect the range of feeding specializations represented by early protocetids.

is virtually identical in comparable parts and in stage of tooth eruption to GSP-UM 3295. It is now identified as the cranium of an immature *Dalanistes* rather than *Remingtonocetus*. Skulls of *Dalanistes* and *Remingtonocetus* can be confused easily, and it is important to know the ontogenetic age of specimens being compared.

Family PROTOCETIDAE Stromer, 1908

Type genus.— *Protocetus* Fraas, 1904a, p. 201.

Included genera.— *Protocetus* Fraas, 1904a, p. 201; *Eocetus* Fraas, 1904b, p. 374; *Pappocetus* Andrews, 1920, p. 309; *Indocetus* Sahni and Mishra, 1975, p. 18; *Babiacetus* Trivedy and Satsangi, 1984, p. 322; *Rodhocetus* Gingerich et al., 1994, p. 844; *Takracetus* Gingerich et al., 1995a, p. 300; *Gaviacetus* Gingerich et al., 1995a, p. 305; *Natchitochia*, Uhen, 1998, p. 664; *Georgiacetus* Hulbert et al., 1998a, p. 912; *Qaisracetus*, new genus.

Diagnosis.— Protocetidae differ from other archaeocetes in having skulls with a broad frontal shield while retaining a full complement of upper and lower teeth (dental formula 3.1.4.3 / 3.1.4.3). Postcranially protocetids have cervical vertebrae intermediate in length between those of remingtonocetids and basilosauroids; generally retain a distinct sacrum composed of one to four vertebrae; first sacral with well developed auricular processes; acetabular notch in pelvis open; femoral head generally has a distinct fovea.

Qaisracetus, new genus

Type species.— *Qaisracetus arifi*, new species.

Included species.— Type species only.

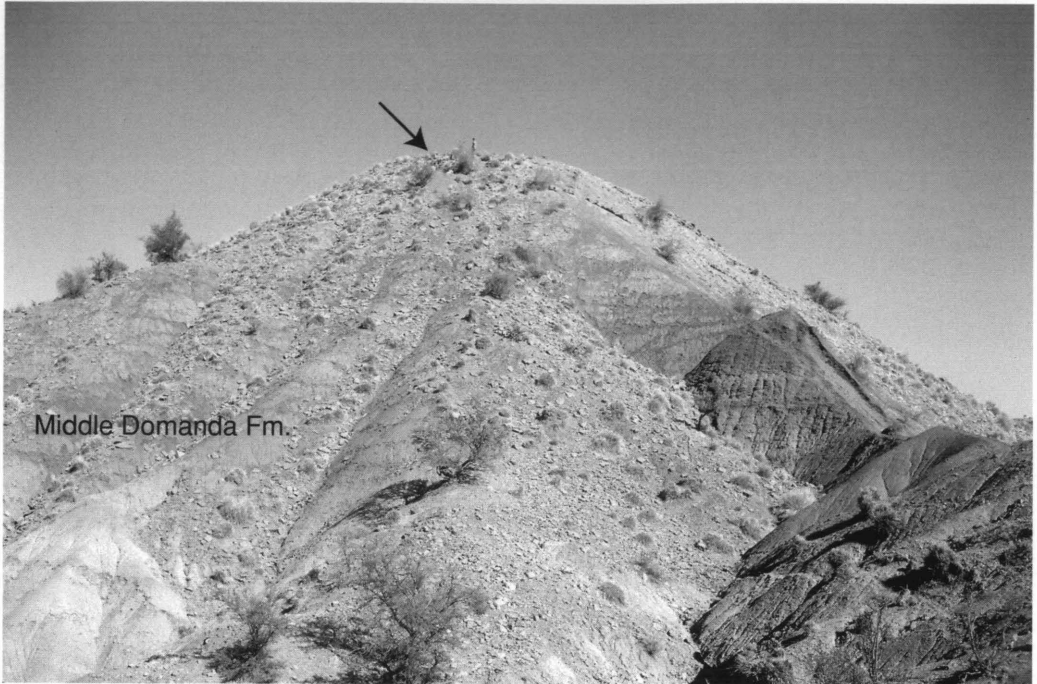


FIG. 19 — Type locality of *Qaisracetus arifi*, new genus and species. Locality of GSP-UM 3410 (holotype; arrow) is in the lower part of the upper Domanda Formation at Ander Dabh Shumali at $30^{\circ} 54.59' N$ latitude and $70^{\circ} 13.77' E$ longitude. View is to the east. Section in foreground includes lower and upper parts of the middle Domanda Formation. The ridge crest above the type locality is formed by limestones in the lower part of the upper Domanda Formation. Men working in the fossil quarry (arrow) and man standing on top of the ridge crest indicate scale.

Diagnosis.— *Qaisracetus* has a generalized protocetid cranium (Fig. 18), with external nares opening above C^1 . It is most distinctive postcranially in having the first two vertebral centra of the sacrum solidly fused, the third joined by pleurapophyses, and the fourth caudal-like and separate, with ventrally-projecting chevron processes. *Qaisracetus* differs from *Takracetus* in having a cranium with a narrower rostrum; differs from *Protocetus*, *Rodhocetus*, *Gaviacetus*, *Natchitochia*, and *Georgiacetus* in retaining solid fusion of sacral vertebrae S1-2; differs from *Eocetus* in lacking pachyostosis of the vertebrae characteristic of the latter; differs from *Pappocetus* in being smaller and having relatively longer cervical vertebrae; differs from *Indocetus* in being larger and having differently shaped upper molars; differs from *Babiacetus* in being smaller, retaining a more distinct protocone on M_1 , and lacking fusion of the mandibular symphysis.

Etymology.— *Qaisra* (*Kisra*, *Qaysar*, *Caesar*, *Czar*, *Kaiser*; title of royalty in Persian and other Indo-European languages), nominal root of the Qaisrani Baloch tribe (sometimes spelled Kasrani) inhabiting Dabh Nala and Karkana; and *ketos*, Gr. (masc.), whale. The name is given to acknowledge the quality of the type specimen, and our appreciation of the substantial assistance and generous hospitality provided by Qaisrani tribesmen during our field work.

***Qaisracetus arifi*, new species**

Figs. 20-24

Holotype.— GSP-UM 3410; including partial cranium; partial dentaries; atlas and several other cervical vertebrae; virtually complete series of well preserved thoracic, lumbar, sacral, and proximal caudal vertebrae; complete left innominate.

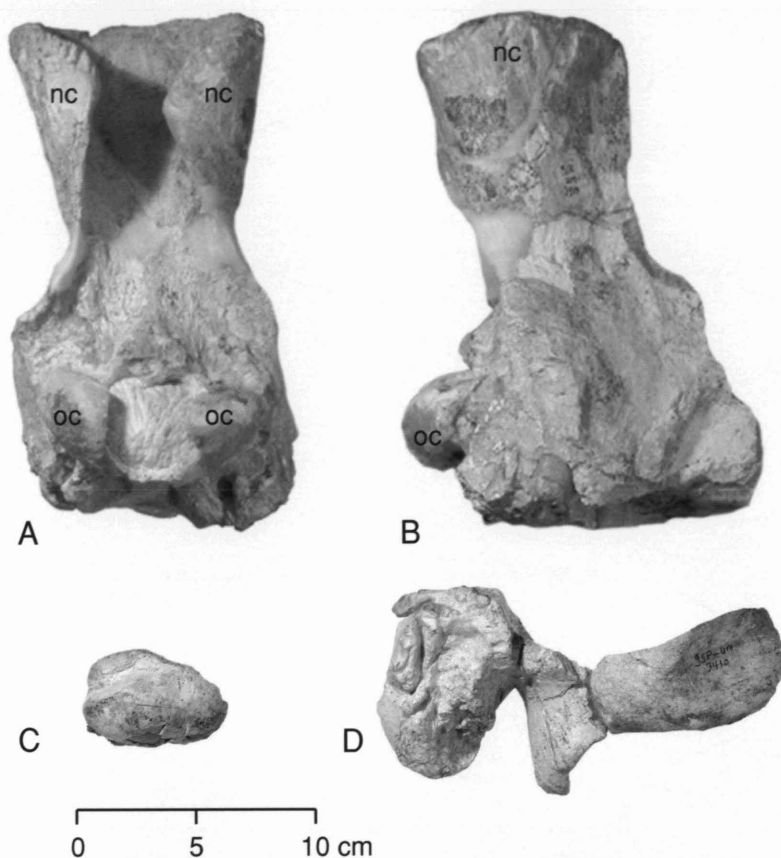


FIG. 20 — Cranial elements of the holotype specimen of *Qaisracetus arifi* (GSP-UM 3410). A-B, Occipital and nuchal area of cranium in posterior and right lateral views. C, right squamosal with glenoid in right lateral view. D, left auditory bulla in ventral view.

Paratype.— GSP-UM 3316, well preserved cranium with associated vertebrae including cervicals and the centrum of a fourth sacral.

Type locality.— Ander Dabh Shumali at 30° 54.59' N latitude, 70° 13.77' E longitude (Fig. 19), near Drug in easternmost Baluchistan Province, Pakistan. The type specimen was recovered from light green shales in the 300-305 m interval, just below the wavy limestone, in the lower part of the upper Domanda Formation. The paratype came from Ander Dabh Janubi at 30° 52.00' N latitude, 70° 13.27' E longitude. This was recovered from the bivalve-filled rubbly marl with oyster shells at the 309.5 m level, just above the wavy limestone, in the lower part of the upper Domanda Formation. Both intervals are early late Lutetian in age.

Diagnosis.— As for the genus.

Hypodigm.— Twelve specimens: GSP-UM 3294, partial skull; 3311, braincase, distal radius and ulna; 3316 (paratype), see above; 3318, distal humerus; 3323, braincase, partial skeleton; 3326, partial scapula; 3327, partial cranium; 3328, partial skeleton (not yet prepared); 3342, posterior thoracic centrum; 3346, caudal centrum; 3407, partial sacrum; and 3410 (holotype), see above. All were found at different localities in Ander Dabh Janubi and Ander Dabh Shumali, and all except GSP-UM 3294 and 3410 (holotype) came from the bivalve-filled rubbly marl yielding the paratype.

Age and distribution.— *Qaisracetus arifi* is found only in the lower part of the upper Domanda Formation, and it is known only in the Ander Dabh Janubi and Ander Dabh Shumali areas near

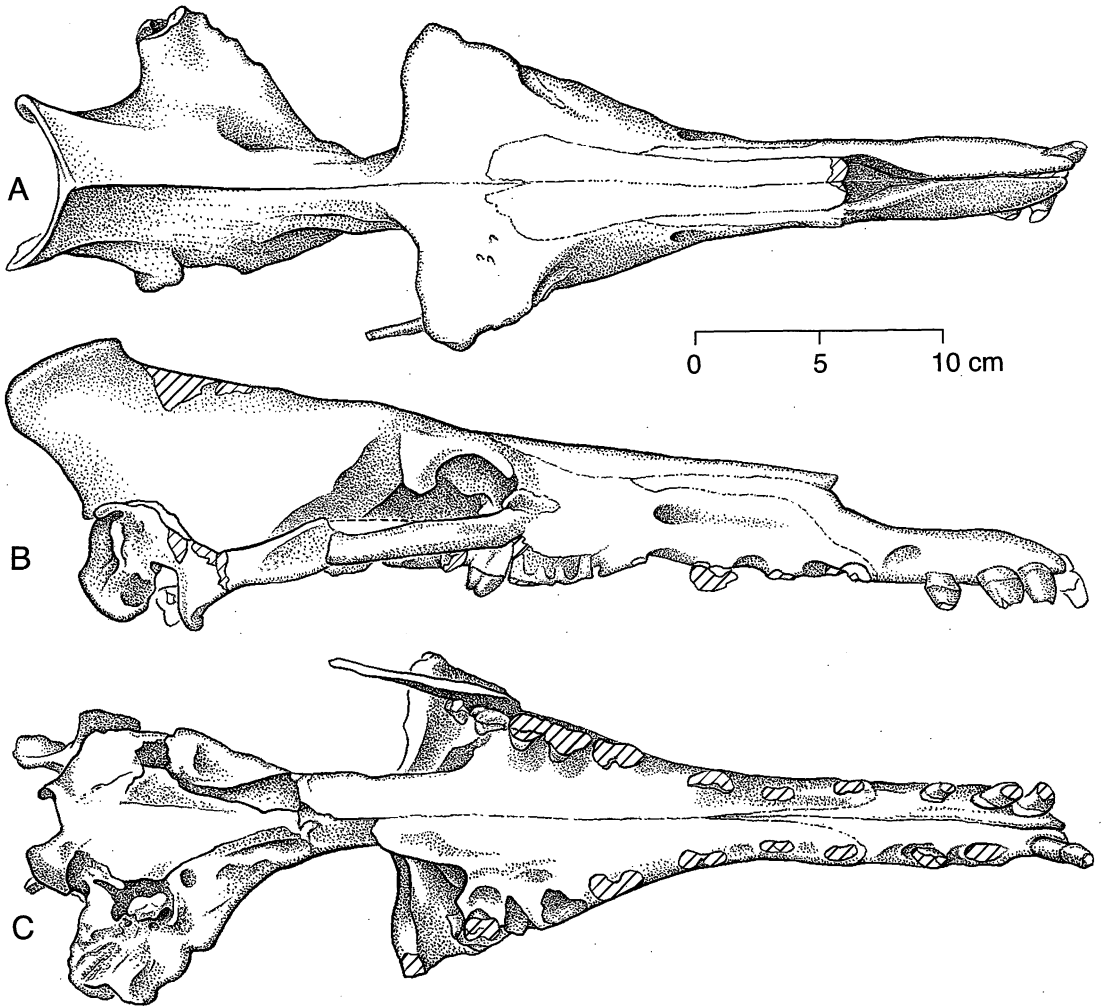


FIG. 21 — Cranium of paratype specimen of *Qaisracetus arifi* (GSP-UM 3316) in dorsal (A), right lateral (B), and palatal (C) views. Note anterior position of the external nares and relatively broad frontal shield.

Drug in eastern Balochistan, Pakistan. The species is early late Lutetian in age, calibrated at approximately 43 Ma (Fig. 11).

Etymology.— Named for Mr. Muhammad Arif, Deputy Director recently retired from the Geological Survey of Pakistan, in recognition of his many contributions to the development of archaeocete paleontology in Pakistan.

General description.— The holotype, GSP-UM 3410, is a partial skull with much of the axial skeleton that was found weathering out in situ. Parts of the cranium, lower jaws, and cervical vertebrae were found on the slope below the rest of the specimen, but the posterior part of the braincase, axis, articulated thoracic, lumbar, sacral, and caudal vertebrae, ribs, and innominate were excavated in place. Several large segments of the axial skeleton were removed in plaster jackets for preparation in the laboratory. Articulated vertebrae of the type specimen were found coiled in a C-shape, presumably due to postmortem contraction of the supraspinous ligament and dorsal epaxial back musculature. This is reminiscent of preservation of *Dorudon* skeletons in Egypt. The paratype, GSP-UM 3316, is a well preserved cranium and associated vertebrae found

TABLE 3 — Measurements of the cranium of the paratype specimen of *Qaisracetus arifi*, GSP-UM 3316. All measurements are in cm. Asterisks denote estimates.

Measurement	A.-p. length or position	Transverse breadth	Height
Skull length (condylobasal skull length: apex–condyles)	64.5		
External narial opening (apex–nares)	16.0		
Posterior extent of nasals (apex–nasal–frontal contact; max. breadth)	39.0	6.8	
Anterior border of orbits (apex–intersection at midline)	37.0	15.5	
Posterior border of frontal shield (apex–intersection at midline)	44.0	21.5	
Junction of sagittal and nuchal crests (apex–intersection at midline)	64.5		
Posterior margin of nuchal crests (apex–intersection at midline)	68.5	11.0	
Second incisor (I ² ; apex–intersection at midline; max. breadth)	6.0	5.2	
First premolar (P ¹ ; apex–intersection at midline; max. breadth)	19.0	5.6	
Last upper molar (M ³ ; apex–intersection at midline; max. breadth)	35.0	15.0	
Internal nares (choanae; apex–intersection at midline; max. breadth)	51.0*	6.5*	
Maximum width of skull (apex–intersection at midline; max. breadth)	55.0*	28.0*	
Squamosal width of skull (apex–intersection at midline; max. breadth)	58.0*	26.5*	
Exoccipital (apex–intersection at midline; max. breadth)	63.0	23.0	
Tympanic bulla length, width, and height	6.5	4.85	4.05
Orbit diameter		4.5	
Foramen magnum width and height		4.4	4.4
Occipital condyles		10.0	3.95
Infraorbital canal, width and height		0.5	1.3
Highest point of nuchal crest above base of occipital condyles			17.5
Highest point of nuchal crest above base of tympanic bulla			21.0*
Dentary maximum length	—		
Mandibular symphysis length (unfused)	—		
Dentary at C ₁ width and height		—	—
Dentary height at position of M ₃			7.2*
Mandibular foramen width and height		2.15*	6.1*

embedded in rubbly marl like other referred specimens. Specimens in this marl were all disarticulated and scattered to some degree before burial.

Skull.— The holotype, GSP-UM 3410, includes the braincase and nuchal crest of a cranium, a squamosal, and an auditory bulla (Fig. 20), and the paratype cranium, GSP-UM 3316, is complete from the tip of the rostrum to the occipital condyles and nuchal crest (Fig. 21). It measures 64.5 cm in condylobasal length, with the maximum width estimated to have been about 28 cm across the zygomatic arches. In terms of proportions, the cranium is similar to those of other early protocetids such as *Protocetus* and *Rodhocetus* (Fig. 18). The rostrum is neither as broad anteriorly as that of *Takracetus* nor as constricted posteriorly as that of *Gaviacetus*. The external nares open relatively far anteriorly, above C¹, the frontal shield is relatively broad, and the nuchal crest is unusually large for a protocetid. The orbits are large, measuring 4.5 cm in diameter. The occiput and nuchal crest are preserved in both the type and paratype specimens. In the type the height of the nuchal crest above the base of the occipital condyles is 21 cm (Fig. 20A,B), while in the paratype this distance is 17.5 cm. The nuchal crest is 11 cm in breadth in both specimens. In the type specimen, GSP-UM 3410, the nuchal crest is very thick, and it is curved posteriorly and medially to the point that left and right flanges of bone almost touch each other. Embrasure pits in the palate to accommodate apical cusps of lower teeth are about equally developed lingual to the anterior portions of P⁴, M¹, and M². Auditory bullae were found with both specimens. These are

relatively small for a protocetid with such a large skull. The infraorbital canal is small and elliptical in cross section, with the longer dorsoventral axis of the ellipse measuring about 1.3 cm. Measurements of the paratype skull are summarized in Table 3.

Upper dentition.—Incisors are present on both sides of the rostrum in the paratype cranium. Right I¹ is displaced posteriorly from its normal position, possibly due to injury in life, while left I¹ may extend a little anterior of its normal position. The root of I¹ is procumbent and the crown appears slightly hooked in the sense of having a tip more down-turned than the rest of the crown. The crown of I² is similar to that of I¹ but slightly larger, while the crown of I³ is similar but notably smaller. The crown of C¹ is not preserved but it appears from the cross section of the root to have been about the same size as I².

P¹ was single-rooted and about the size of I³. P² and P³ were double-rooted. A part of the crown of right P² is present, but this shows only that there was a weak lingual cingulum on upper premolars. The posterior root of P³ is expanded lingually, indicating slight development of a posterolingual protocone ridge on the crown of P³. The base of the crown of P⁴ is present on the right side, and P⁴ appears to have had a separate third root on the lingual side supporting the lingual protocone ridge. This was more centered on the lingual side of the tooth than that of P³. There is a distinct lingual cingulum on P⁴ and there are three small beads of enamel on the crown just distal to this.

The base of the crown of M¹ is present on the right side of the palate in the paratype. This tooth was three-rooted. The protocone ridge on M¹ is a little broader than that on following molars, and it is a little more flattened near its base. The enamel at the base of this ridge is perforated by wear in a way that suggests a distinct protocone cusp or swelling of enamel was probably present. There is a faint lingual cingulum on M¹, following the lingual margin of the tooth. Starting at the front, this margin curves smoothly from concave lingually in front of the protocone to convex lingually around it.

The crown of M² is virtually complete and it too was three-rooted. M² was found displaced slightly from its natural position in life, which helped to preserve it. The paracone is the largest cusp, and there is a smaller but substantial metacone directly behind this. Together the two labial cusps form a small carnassial notch. The apex of the paracone is worn off obliquely, and there is a long, narrow, smoothly-polished wear facet running down the anterolingual surface of the paracone connecting the apex to the base of the crown. A beaded lingual cingulum is prominent anterior to this, weakly expressed where the wear facet crosses it, and then again well developed lingual to the protocone ridge. There is a prominent posterolingual protocone ridge lingual to the metacone, with a small flat wear facet in the position where a protocone cusp might have been located, but there is no clear indication that such a distinct cusp was present. The anterior crest of the paracone and the posterior crest of the metacone are finely but distinctly serrated. There is a weak but distinct cingulum bordering the labial base of the crown.

The right M³ was broken from the maxilla at the time of burial and found floating in sediment filling the right temporal opening. There is no position for an M³ evident on either side of the palate, and if the tooth had not been found it might have seemed that no M³ was present at all. However, the tooth was found and it is clear that *Qaisracetus* had three upper molars. M³ was possibly three-rooted, but the only substantial root is the lingual or protocone root. The crown is smaller than that of M², with probably a single apical cusp (there is a distinct cusp near the posterior base of the crown that may be homologous with the metacone). There is a continuous cingulum surrounding both the labial and lingual bases of the crown. There is again a flat wear facet crossing the posterolingual surface of the crown in the position of a protocone, but there is no distinct protocone cusp.

Measurements of upper teeth are listed in Table 4.

Dentaries.—Fragments of both dentaries were found with the type specimen. These show that left and right mandibles were unfused. A natural stone endocast in the paratype shows mandibular canal height to have been 6.1 cm near the opening of the mandibular foramen. Farther forward the mandibular canal is only 2.1 cm high and 1.7 cm wide beneath the posterior root of P₃. Lower teeth are not known.

TABLE 4 — Measurements of teeth in the paratype specimen of *Qaisracetus arifi* GSP-UM 3316. Measurements in parentheses are based on alveoli. All measurements are in mm. Asterisks denote estimates.

Tooth position	Crown length	Crown width	Apical height	Trailing diastema
<i>Upper dentition</i>				
I ¹	22.5	13.6	29.0*	10.0
I ²	24.4	13.6	—	11.8
I ³	20.0	11.8	16.0*	33.5
C ¹	(23.0)	(13.5)	—	18.5
P ¹	(22.0)	(11.0)	—	20.0
P ²	(31.8)	(14.0)	—	28.0
P ³	(32.0)	(20.8)	—	3.5
P ⁴	27.5	23.1	—	0.0
M ¹	22.2	22.0	—	0.0
M ²	23.4	20.0	21.2	0.0
M ³	15.5	18.0	—	—

Vertebrae.— Vertebrae are preserved in the holotype, paratype, and other referred specimens. Those described here are from the holotype, GSP-UM 3410, unless otherwise noted. Vertebrae of the holotype were preserved in articulation, with only the cervicals being disturbed by erosion, meaning that vertebral counts and identifications to position within the series are known with certainty. In the referred specimens vertebrae were found associated but disarticulated, and most can only be identified to position by reference to the holotype.

The cervical series is not known completely, but all or part of five of the seven vertebrae are represented. The most complete is the first cervical, the atlas or C1, of the holotype (Fig. 22A,B). This has no centrum per se, but a large ring of bone enclosing a keyhole-shaped central space, the upper part of which is the neural canal, flanked anteriorly by confluent surfaces for articulation with the occipital condyles of the cranium. These are bridged dorsally by a relatively thin and flat neural arch. Posteriorly the neural canal is flanked by left and right surfaces, almost flat, for articulation with corresponding surfaces of the following axis vertebra or C2. These axial facets are separated by the articular surface for the dens of C2, which floors the medial part of the central space below the neural canal, and by a robust hypapophysis projecting posteroventrally on the midline. The neural arch is more arched in posterior view than it is in anterior view. There are massive posterolaterally directed wings of bone or alae flanking the axial facets. These are concave anteriorly, and each wing ends in two prominent bosses, one ventral and one dorsal. The vertebral artery passed through three distinct foramina in the atlas before entering the foramen magnum of the skull. The artery first passed through a transverse foramen in the posterior or more vertical surface of the ala to enter the concave space in front, then it passed through a second foramen in the coronal surface of the ala to reach the dorsal surface of the atlas, then it passed through the intervertebral foramen proper to enter the dorsal part of the keyhole-shaped central space.

The axis (C2) is represented by a part of the neural arch only. This is robust, and is distinctive in having a relatively short, blunt neural spine with a broad, flat surface for insertion of the nuchal ligament, rather than the long and more pointed spine often seen in protocetids. C3 and C4, represented by centra only, are identifiable by the presence of a large hypophysis, and by the position of the vertebralarterial canal impressed in the lateral margin of each centrum. The arterial canal is higher on the centrum of C3 than it is on that of C4. The centrum of C6 is notable in preserving the robust base of a ventrally-deflected transverse process that must have been massive. Centra of all three of these vertebrae are intermediate in shape between those of remingtonocetids with relatively longer centra and basilosaurids with relatively shorter centra.

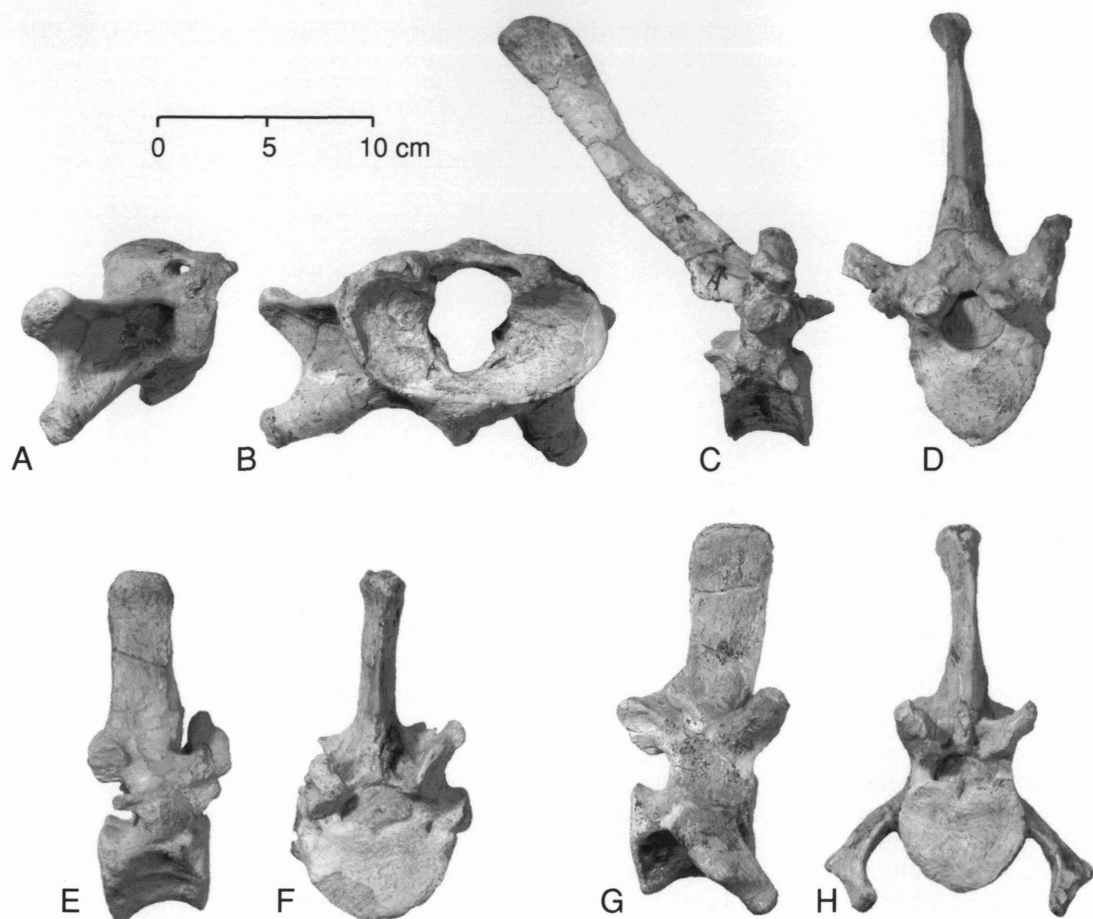


FIG. 22 — Representative vertebrae of the holotype specimen of *Qaisracetus arifi* (GSP-UM 3410). A-B, atlas vertebra (C1). C-D, sixth thoracic vertebra (T6). E-F, twelfth thoracic vertebra (T12). G-H, third lumbar vertebra (L3). Each is shown in anterior and right lateral views, respectively. Note massive transverse processes on C1, high neural spine on T6, short and straight neural spine on T12 (anticlinal vertebra), and revolute prezygapophyses on L3.

The holotype includes a complete series of 13 well preserved thoracic vertebrae. T6, T11, and T12 are representative and described here in detail. In T6 (Fig. 22C,D) the anterior surface of the centrum is pentagonally curved in outline and slightly convex. The shortest side of the outline underlies the neural canal, longer sides flank this, underlying the capitular facets for ribs, and the longest sides join at the ventral midline. The posterior surface is more heart-shaped, and slightly concave. This is flanked dorsolaterally by capitular facets for ribs. There is no ventral keel on the centrum but some lipping anteriorly and posteriorly for attachment to a ventral longitudinal ligament. The neural canal is eccentric in cross-section, being narrower dorsally than it is ventrally. Pedicles are massive, supporting thick laminae of the neural arch and robust transverse processes. Transverse processes arise from the lateral surfaces of the pedicles rather than the centrum. Prezygapophyses are almost flat, and slope slightly downward both anteriorly and laterally. Postzygapophyses are also almost flat, and slope slightly upward both posteriorly and medially. There is a single broad pit between each pair of pre- and postzygapophyses for a strong interspinous ligament. Each transverse process has a large oval tubercular facet for articulation with rib tubercles, and a robust metapophysis rises above this. There is a distinct fovea at the poste-

rolateral base of each metapophysis for origination of a dorsocostotransverse ligament. The neural arch is broad and relatively flat at its base, tapering rapidly to a long spine. The spine has a distinct thickening at its apex for attachment of a supraspinous ligament.

T11 (Fig. 22E,F) is generally similar to T6 but the centrum is longer and broader, the distance between capitular and tubercular rib facets is smaller, the metapophyses are lower, and the neural spine is shorter and more vertical. T11 is of particular interest in having prezygapophyses almost flat and sloping slightly downward both anteriorly and laterally like those of more anterior thoracics, while postzygapophyses are slightly revolute and oriented steeply upward, facing laterally and only slightly downward. This difference between pre- and postzygapophyses means T11 is clearly and distinctly diaphragmatic.

T12 is similar in size and shape to T11, but different in detail. T12 has the steeply oriented and slightly revolute prezygapophyses characteristic of more posterior thoracics and lumbar. There is a single facet on the transverse process rather than on the body of the centrum for articulation with the capitulum of the corresponding rib (there is no tubercular facet), and the metapophyses arise from the laminae of the neural arch in association with the prezygapophyses rather than from the transverse processes. The transverse processes have distinct posteriorly-oriented spines or anapophyses not seen in more anterior vertebrae. There is a distinct pit on each side of the base of the neural spine for separate left and right interspinous ligaments. Finally, the neural spine of T12 is the first to rise parallel to the articular surfaces of the centrum rather than sloping backward, and this is consequently the anticlinal vertebra.

The holotype includes a complete series of six well preserved lumbar vertebrae. L3 is representative and described here in detail (Fig. 22G,H). The centrum is longer and more cylindrical than those of preceding vertebrae. The anterior surface of the centrum is slightly convex while the posterior surface is almost flat. Both of these surfaces are heart-shaped to circular in outline, but the posterior surface has distinct ventrolateral corners suggesting attachment to a well developed ventral longitudinal ligament. Transverse processes arise from lateral surfaces of the centrum and curve outward, downward, and forward to distinct 'elbows' before turning inward, downward, and forward. Metapophyses arise from the anterior surfaces of laminae of the neural arch. These have prezygapophyses on their inner surfaces, with articular surfaces steeply inclined and moderately revolute rather than flat. Postzygapophyseal processes arise from the posterior surfaces of laminae of the neural arch, with articular surfaces steeply inclined and moderately revolute. The neural spine is robust, forwardly-inclined slightly, and both longer anteroposteriorly and higher dorsally than those of preceding posterior thoracic vertebrae. As before, the spine has a distinct thickening at its apex for attachment of a supraspinous ligament.

The sacrum, comprising four vertebrae, is virtually complete in the holotype, GSP-UM 3410 (Fig. 23A-C). Centra of the anterior two vertebrae, S1 and S2, are solidly fused with no trace of a suture between them, as are the connecting zygapophyses and portions of the laminae. S1 has the highest neural spine of the sacrum, the highest metapophyses, and transverse processes with expanded auricular surfaces for articulation with the innominate. S2 has a slightly lower neural spine. The transverse process on S2 is broad and flat, joined to that of S1 by a pleurapophyseal synostosis, and to that of S3 by a pleurapophyseal synchondrosis. Pedicles of S1 and S2 enclose a dorsal sacral foramen, and transverse processes of S1 and S2 enclose a pelvic sacral foramen. These foramina transmit sacral nerves and blood vessels. The zygapophyseal articulations between S2 and S3 are normal and the centra were separated by an intervertebral disk, but S3 is unmistakably sacral because of its pleurapophyseal articulation with the transverse process of S2 (not preserved on S3 but evident on S2).

It does not appear that S4 had pleurapophyses, nor were there special articulations of any kind with the preceding vertebra. S4 would undoubtedly be considered a caudal except for the presence of distinctive left and right ventral processes projecting posteriorly from the centrum. These hemal processes evidently developed to partially surround the median coccygeal artery. Anterior caudal vertebrae have articular facets in this position for hemal arches, and development of ventral processes here serving the same function suggests that the processes are neomorphs developed on a partially caudalized S4 rather than Ca1.

The holotype includes a partial series of six well preserved caudal vertebrae. These were found in articulation with the rest of the vertebral column and represent Ca1 through Ca6. Each caudal has a corresponding hemal arch or chevron bone found in articulation with it. Ca3 is representative and described here in detail (Fig. 23E,F). The longest vertebrae found in the *Qaisracetus* skeleton are caudals, and the centrum of Ca3 is long. The anterior surface of the centrum is almost circular in outline and convex. The flat part of the outline is at the top where the centrum borders the neural canal. The posterior surface of the centrum is distinctly hexagonal, with each side of the hexagon being approximately equal. The dorsal surface is again flat where the centrum borders the neural canal, and the ventral border of the outline appears flat because of expansion of the posterior ventrolateral corners into facets for articulation of the hemal arches. The transverse processes are substantial and project almost directly laterally, curving downward and slightly backward. The pedicles of the neural arch are more than half the length of the centrum. They enclose a relatively broad and flat neural canal. The metapophyses arise from the neural arch itself. Each is both long anteroposteriorly and high, curving laterally and upward. The prezygapophyses are flat surfaces on the medial sides of the metapophyses. The neural spine is approximately vertical. It rises higher than the metapophyses but is much less substantial. Postzygapophyses project posteriorly from the neural arch or base of the neural spine.

Caudal chevrons associated with Ca1 through Ca6 in the holotype are all similar in having left and right arms articulating dorsally with corresponding chevron facets at the posterior ventrolateral corners of caudal vertebrae. These arms enclose a hemal canal and are fused distally to form a hemal spine. The chevron associated with Ca3 encloses a hemal canal measuring about 1.8 cm in width and 2.5 cm in depth. The dorsoventral projection of the whole arch is about 6.0 cm and the anteroposterior length of the spine is about 3.5 cm.

Measurements of all of the vertebrae present in the holotype are listed in Table 5.

Ribs.— Many partial ribs and pieces of ribs were collected with the holotype. None can be identified to position precisely. All are typical for early protocetids in being relatively slender with slight distal expansion. There is no indication of osteosclerosis nor of pachyostosis. The most complete is a rib from the anterior to middle part of the thorax estimated to have been about 35 cm long when complete. This has a head measuring 2.05×1.65 cm, a neck measuring 1.68×1.35 cm, the caput and tuberculum well separated (ca. 4 cm on centers), a tuberculum measuring 2.08×1.75 cm, a curvature of radius about 5 cm at its tightest, a distinct crest at the angle of the rib, and a gently curved body measuring about 2.0×1.5 cm at midshaft. Another piece of rib measures 2.37×1.48 cm at midshaft, and 2.90×2.38 cm at the slightly expanded distal end.

Innominate.— The left innominate is well preserved in the holotype (Fig. 23D). It was found in situ and excavated from a position close to the posterior part of the skull, approximately 1.5 m from the sacrum. The right innominate was not found. Hence it is clear that both innominates were displaced before the skeleton was buried. Salient features of the innominate are its long ilium with a roughened surface for articulation with the auricular process of the sacrum; well-formed acetabulum with a well-formed lunate surface and distinct acetabular notch; large obturator foramen; and roughened pubic symphysis for articulation with the opposite innominate. It is similar in size and shape to that of *Georgiacetus* (Hulbert et al., 1998), but differs most importantly in retaining clear evidence of direct articulation with the sacrum.

The ilium is long and relatively straight, with the dorsal iliac spine expanded anteriorly. The inner side of this dorsal expansion is a roughened articular surface that matches the auricular process of the sacrum and there is no doubt that the innominates and sacrum formed a unified pelvis. The ilium has a distinct triangular pit for origination of ligaments or muscles just in front of the acetabulum, and there is a prominent iliopectineal eminence on the ventral border of the ilium. The pubis is about two-thirds the length of the ilium. It has a relatively narrow ramus bordering the obturator foramen and a distinct pubic tubercle near the midline. The broadest part of the pubis is the part separating the obturator foramen from the pubic symphysis. The pubic symphysis itself is shallow and relatively long anteroposteriorly. Dorsal and posterior rami of the ischium are broader than the pubic ramus. The posterior ramus with its counterpart from the right side formed

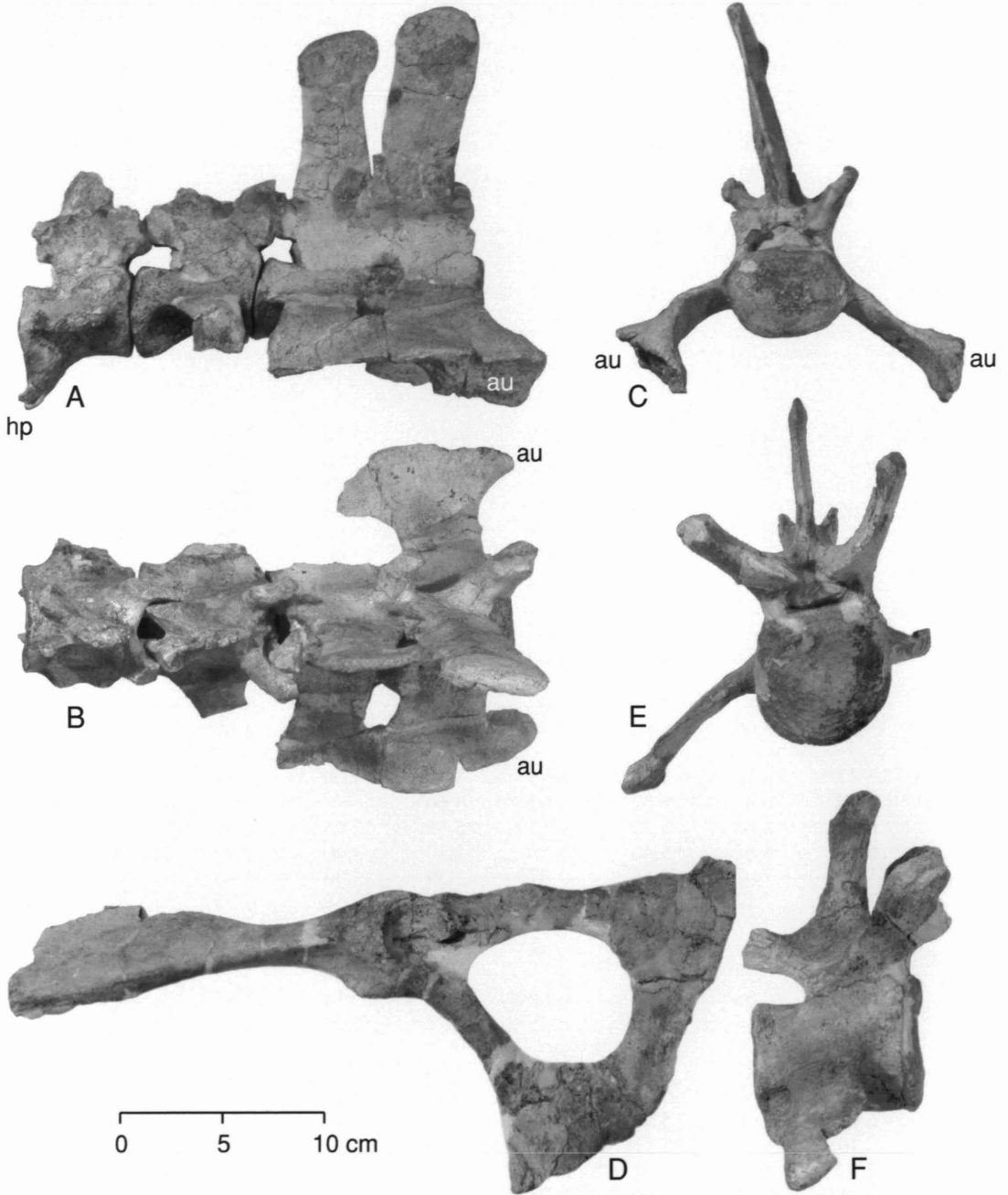


FIG. 23 — Sacrum, innominate, and representative caudal vertebra of holotype specimen of *Qaisracetus arifi* (GSP-UM 3410). A-C, sacrum with four sacral vertebrae (S1 through S4) in right lateral, dorsal, and anterior views. D, left innominate in left lateral view. E-F, third caudal vertebra (Ca3) in anterior and right lateral views.

a broad midline ischiatic notch or arch. There is a thin but distinct ischiatic tuberosity at the posterior apex of the ischium.

TABLE 5 — Measurements of vertebrae in the holotype specimen of *Qaisracetus arifi* GSP-UM 3410. All measurements are in cm, except neural spine angle (degrees, measured backward from vertical). Asterisks denote estimates. Abbreviations: *ant. hgt.*, anterior height; *ant. wid.*, anterior width; *neur. can.*, neural canal; *neur. sp.*, neural spine; *pos. hgt.*, posterior height; *pos. wid.*, posterior width.

Vertebra	Centrum length	Centrum ant. wid.	Centrum ant. hgt.	Centrum pos. wid.	Centrum pos. hgt	Neur. can. width	Neur. can. height	Neur. sp. height	Neur. sp. angle (°)
<i>Cervix</i>									
C1	2.95	—	—	7.00*	4.40	3.97	4.20	0.00	—
C2	—	—	—	—	—	2.33	—	6.00*	+20
C3	3.28	4.54	4.09	4.55	4.44	2.43	2.06	—	—
C4	3.35	4.69	4.54	4.72	4.48	2.49	1.97	—	—
C5	—	—	—	—	—	—	—	—	—
C6	3.52	4.48	4.12	5.12	4.12	—	—	—	—
C7	—	—	—	—	—	—	—	—	—
<i>Thorax</i>									
T1	4.20	4.60	4.28	5.50	4.40	3.30	2.50	14.00	+20
T2	4.38	5.15	4.77	6.15	4.65	3.20	2.20	—	+38
T3	4.40	5.47	4.82	5.48	5.33	2.84	2.27	18.00	+46
T4	4.45	6.00	5.05	5.80	4.95	2.84	2.08	20.00	+42
T5	4.45	5.28	4.85	6.12	4.90	2.88	2.68	19.00	+41
T6	4.32	5.43	4.59	5.80	4.54	2.96	2.69	18.30	+44
T7	4.19	5.37	4.27	5.78	4.54	2.93	2.72	16.20	+46
T8	4.34	5.15	4.53	5.65	4.54	—	—	—	—
T9	4.58	5.43	4.50	5.62	4.85	3.08	2.36	14.00	+48
T10	4.64	5.88	4.59	5.89	—	3.13	2.47	12.00	—
T11	4.86	6.09	4.70	6.60	5.00	—	—	—	+30
T12	4.93	6.84	4.78	7.02	4.84	3.40	2.20	10.50	+03
T13	5.15	6.00	4.80	6.64	5.44	3.12	1.69	11.00	-05
<i>Lumbus</i>									
L1	5.47	6.20	5.05	6.89	5.84*	3.00	1.53	11.00	-15
L2	5.69	6.38	5.52	7.02	5.60	—	—	—	—
L3	6.04	6.55	5.72	7.15	5.58	2.96	1.66	11.50	-07
L4	6.60	6.67	5.46	7.50	5.40	3.40	1.40	12.00	-18
L5	7.00	7.02	5.38	7.87	5.39	3.90	1.40	12.50	-15
L6	7.09	7.12	5.26	7.60	5.26	3.58	1.75	13.20	-13
<i>Sacrum</i>									
S1	7.00	7.29	5.14	6.98	—	3.20	1.88	13.50	-03
S2	6.50	6.98	—	—	5.06	—	—	—	—
S3	6.90	6.60	4.76	6.69	5.35	3.15	1.32	—	—
S4	6.62	6.48	5.15	6.25	5.71	2.90	1.13	—	—
<i>Cauda</i>									
Ca1	6.55	5.83	5.73	6.05	6.00	2.43	1.12	—	—
Ca2	6.90	5.66	5.99	6.14	6.10	2.40	1.12	—	-05
Ca3	6.90	5.60	5.82	6.05	6.33	2.45	0.93	7.50	-0
Ca4	7.40	5.38	6.11	6.12	6.29	2.33	0.90	—	-05
Ca5	7.70	5.88	5.98	6.31	6.07	1.88	0.70	—	-0
Ca6	7.71	6.01	5.90	6.03	6.20	1.70	0.65	—	-0

Measurements of the innominate are listed in Table 6.

Limb bones.— Pieces of four limb bones, all from the forelimb, are preserved in three specimens. GSP-UM 3326 is a piece of a distal right scapula preserving much of the glenoid and base of the acromion. The glenoid is elliptical outline, measuring approximately 4.25×5.45 cm, and the neck above this measures about 5.3×1.7 cm at the base of the acromion.

TABLE 6 — Measurements of the left innominate preserved in the holotype specimen of *Qaisracetus arifi* GSP-UM 3410. All measurements are in cm. Asterisks denote estimates.

<i>General</i>		
Maximum length of entire innominate	42.8	
Obturator foramen, maximum and minimum diameters	9.7	7.5
<i>Ilium</i>		
Ilium length, maximum breadth above acetabulum	23.5	3.2
Ilium minimum dorsoventral height, transverse width at this point	2.5	2.1
Iliac spine height, thickness	6.6	0.7
Iliac spine auricular surface height, anteroposterior length	4.1	11.7
<i>Ischium</i>		
Ischium length	19.3	
Dorsal ramus of ischium, maximum and minimum diameters	2.6	1.1
Ventral ramus of ischium, maximum and minimum diameters	3.1	1.3
<i>Pubis</i>		
Pubis length	16.0	
Ramus of pubis, maximum and minimum diameters	2.1	1.3
Pubic symphysis, maximum and minimum diameters	8.0	1.4
<i>Acetabulum</i>		
Acetabulum diameter	3.8	

GSP-UM 3318 is the distal half of a robust humerus. This appears to have been about 20 cm in total length. It measures 4.5 cm anteroposteriorly and 2.72 cm mediolaterally at midshaft. The maximum width of the distal end is 5.8 cm. Distinctive characteristics are the presence of an elliptical area of cancellous bone measuring about 2.2×1.8 cm in cross-section exposed where the bone is broken at midshaft. There is a 0.45 cm thickness of cortical bone surrounding this anteriorly, medially, and laterally, but posterior to this the humeral cross-section is expanded with a ca. 1.85 cm thickness of dense cortical bone. This is reminiscent of the thick cortical bone of the expanded deltopectoral crest on the humerus of *Dorudon*, but differs in lying on the back rather than on the front of the humeral shaft. The olecranon fossa is deep but not perforated. The trochlea of the humerus is distinctly V-shaped, with a minimal diameter in the trough of the V of about 2.85 cm and a maximum diameter medial to this of about 3.4 cm. The articular surface is not complete, but what is preserved appears to have been eccentric, suggesting some habitual flexion of the elbow and a limited range of flexion and extension.

GSP-UM 3311 includes the weathered distal ends of both a radius and an ulna. The distal radius measures 3.75×3.00 cm in maximum and minimum transverse diameter where it is thickest, and the distal surface has two circular facets of about 1.6 cm diameter positioned side by side. The distal ulna measures about 2.55×2.15 cm in maximum and minimum transverse diameter at the position of the fused epiphyseal suture. This has a single elliptical facet of about the same maximum diameter as the facets on the radius. Both ulna and radius have some of what must have been a thin layer of cortical bone weathered off to expose a core of cancellous bone.

Discussion.— It is easy to speculate about the locomotor and other adaptations of archaeocetes for life in water, but such speculation has little basis without evidence provided by associated and preferably articulated skeletons. The most complete articulated skeleton of a protocetid described to date is that of *Rodhocetus kasranii* from the early Lutetian of the Rodho anticline near Satta Post in the eastern Sulaiman Range of Punjab (Gingerich et al., 1994). *Rodhocetus kasranii* is relatively advanced evolutionarily in having a sacrum lacking fusion of successive centra but it is primitive in retaining pleurapophyses connecting all sacral vertebrae. *Qaisracetus arifi* described here from the late Lutetian is almost identical in skeletal completeness, but contrasts in retaining some sacral fusion while losing all special connections between other sacral vertebrae. Each is differently specialized, and it is not clear which is more likely to be on the main line of later whale evolution. Both are important in documenting the length and form of much of a vertebral column, but neither is complete and there is a limit to what we can say about their locomotion.

One approach to interpretation of protocetids involves construction of diagrams of skeletal proportion comparing skull, vertebral, and limb lengths and proportions, scaled to facilitate comparison of elements within the same skeleton and comparison of skeletal proportions across taxa. Extant whales and even fully aquatic basilosaurid archaeocetes have very different vertebral profiles from those of land mammals when compared in such diagrams (Gingerich, 1998). Here we introduce an innovation, which is addition of neural arch and neural spine heights for vertebrae to give a more complete picture of skeletal proportions. The skeleton of *Qaisracetus arifi* is compared to that of *Rodhocetus kasranii* in Figure 24. The former has a body weight estimated at about 620 kg, while the latter is slightly smaller with a body weight estimated at about 590 kg. Both have shorter cervicals than are typically found in land mammals but longer cervicals than are found in later whales. Both have anterior thoracic centra that increase slightly in size, with neural spines that increase distinctly in length over the shoulder girdle (stippled box below anterior thoracics). This appears as an arch in a diagram of skeletal proportion. Both have a second such arch in the vertebral column in the lumbosacral region. *Qaisracetus arifi* has anterior caudal vertebrae that lengthen posteriorly, while *Rodhocetus kasranii* has anterior caudal vertebrae that shorten posteriorly. Generalized land mammals, extant wolves for example, have skeletal proportions including similarly separate anterior thoracic and lumbosacral arches in neural spine height. These might be interpreted as skeletal indicators of terrestrial locomotion, but any such interpretation is probably premature until limbs are known for both genera.

The configuration of sacral vertebrae is so different in different genera across the suborder Archaeoceti and so important for understanding hind limb reduction in early whale evolution that a system is required to encode it. Here a convention is proposed using symbols available on any standard keyboard: # represents complete fusion of adjacent centra; = represents the presence of pleurapophyseal contacts in the absence of centrum fusion; and + represents a freely articulating vertebra considered part of a sacrum. Hence the sacral formula of *Qaisracetus* is $S1\#S2=S3+S4$. Sacral formulae for other archaeocetes are listed in Table 7. If the primitive formula for archaeocetes is $S1\#S2\#S3\#S4$, then, as mentioned above, $S1\#S2=S3+S4$ seen here in *Qaisracetus* can be viewed as being specialized in a different way than $S1=S2=S3=S4$ seen in *Rodhocetus*. Retention of a single sacral vertebra, $S1$, as is seen in *Gaviacetus* and *Protocetus* is a further specialization that may have been derived with approximately equal likelihood from the formula of *Rodhocetus* or that of *Qaisracetus*. Even this becomes lost in later archaeocetes, possibly in *Georgiacetus*, and certainly in *Dorudon* and *Basilosaurus*.

STRATIGRAPHIC DISTRIBUTION OF LUTETIAN ARCHAEOCETES IN THE SULAIMAN RANGE

We have now studied the Habib Rahi and Domanda formations and searched for whales in five areas of the eastern Sulaiman Range: near Satta and near Dalana at the north and south ends of the Zinda Pir anticlinorium (Gingerich et al., 1993, 1994, 1995a), and near Drug in the north (this study), near Rakhi Nala (e.g., Wells, 1984; Gingerich et al., 1998), and in the vicinity of Chachar Nala in the south (unpublished). Most of the marker beds illustrated here can be recognized throughout this geographic area. The best exposures studied in detail are those near Drug documented here, where the 62 m thick Habib Rahi Formation in the Chuk Dabh Janubi section (Fig. 3) and the 366 m thick Domanda Formation in the Zuli Khan Sham section (Fig. 5), taken together, clearly show three cycles of lithological change that can be related to the global pattern of sea level rise and fall. Micropaleontological age control is provided by studies in Rakhi Nala (Fig. 11).

The Habib Rahi and Domanda formations together appear to span virtually all of Lutetian middle Eocene time, an interval of about 8 m.y. from about 49 Ma to 41 Ma. Ten superposed stratigraphic intervals in the Habib Rahi and Domanda formations are known to yield archaeocete whales (numbered 1 through 10 in Figs. 3 and 5). Some of these intervals are relatively thin and represent relatively little time, like the interval just above and below the wavy limestone producing *Qaisracetus arifi* described here, while others are thicker and may represent intervals on the order

TABLE 7 — Sacral formulae of selected archaeocetes. *Qaisracetus* illustrates the three possible stages of sacral fusion observed here: #, full fusion of centrum, zygapophyses, and pleurapophyses of successive sacrals (e.g., between S1 and S2 in *Qaisracetus*); =, synchondrosis between pleurapophyses of successive sacrals but no centrum or zygapophyseal fusion (e.g., between S2 and S3); and +, vertebrae identified as sacral but lacking centrum or zygapophyseal fusion and lacking pleurapophyses (e.g., between S3 and S4). Question marks indicate uncertainty. When multiple symbols are used to connect vertebrae (e.g., between S3 and S4 in *Dalanistes*), the connection is known to be variable in different individuals. Sacrals identified as S1 all have expanded auricular surfaces on transverse processes for articulation with innomines. *Basilosaurus* and *Dorudon* lack vertebrae with distinctive characteristics enabling them to be identified as sacral, and this appears to be the case in *Georgiacetus* as well.

Taxon	Reference	Formula
Basilosauridae		
<i>Basilosaurus isis</i>	Gingerich et al. (1990)	No sacrum
<i>Dorudon atrox</i>	Gingerich and Uhen (1996)	No sacrum
Protocetidae		
<i>Georgiacetus vogtlensis</i>	Hulbert (1998)	No sacrum?
<i>Natchitochia jonesi</i>	Uhen (1998)	S1
<i>Protocetus atavus</i>	Fraas (1904a)	S1
<i>Gaviacetus razai</i>	Gingerich et al. (1995a)	S1
<i>Rodhocetus kasranii</i>	Gingerich et al. (1994)	S1=S2=S3=S4
<i>Takracetus simus</i>	GSP-UM 3147	S1#S2=S3+?
<i>Qaisracetus arifi</i>	This paper	S1#S2=S3+S4
Remingtonocetidae		
<i>Remingtonocetus domandaensis</i>	This paper	S1#S2#S3=S4
<i>Dalanistes ahmedi</i>	Gingerich et al. (1995a)	S1#S2#S3#=#S4
<i>Andrewsiphius sloani</i>	Bajpai and Thewissen (2000)	S1#S2#S3#S4

of a million years or so in duration. Much remains to be learned about Lutetian whale evolution, and discovery that the Habib Rahi and Domanda formations of Pakistan are richly fossiliferous opens a unique opportunity for studying this. There is no other setting where such a thick sequence of sedimentary rocks spans such a long duration that is so well exposed for examination, so well dated, and so rich in archaeocetes.

ACKNOWLEDGMENTS

We thank Director General Hasan Gauhar and Directors Abdul Latif Khan, S. Ghazanfar Abbas, and Imran Khan, Geological Survey of Pakistan, Quetta, for encouragement and logistical support in the field. Mr. Muhammad Arif, Deputy Director recently retired from the Geological Survey of Pakistan, honored here in the name of our most complete archaeocete *Qaisracetus arifi*, contributed greatly to organization and execution of field work in the Drug area. Messrs. Malik Ramthulla Jaffar, Jamidar of Drug, and Ramthulla Qaisrani, Sadar of Karkana, deserve special thanks for accommodation and generous hospitality during our field work in Drug Lahar. We thank Prof. Ashok Sahni for access to the types and other specimens of archaeocetes from Kutch stored at Lucknow University, Dr. Kishor Kumar for good casts of many of these, and Dr. J. G. M. Thewissen for an opportunity to see the type of *Kutchicetus minimus*. Specimens described here were prepared by William J. Sanders and Joseph Groenke at the University of Michigan. Drawings in Figure 21 are by Bonnie Miljour, and we thank her for final preparation of all of the illustrations for publication. Drs. Jon I. Bloch, Gregg F. Gunnell, and William J. Sanders read and improved the manuscript. Field and laboratory research was supported by National Science Foundation grant EAR-9714923.

LITERATURE CITED

- AFZAL, J. 1996. Late Cretaceous to early Eocene foraminiferal biostratigraphy of the Rakhi Nala area, Sulaiman Range, Pakistan. *Pakistan Journal of Hydrocarbon Research*, Islamabad, 8: 1-24.
- ANDREWS, C. W. 1920. A description of new species of zeuglodont and of leathery turtle from the Eocene of southern Nigeria. *Proceedings of the Zoological Society of London*, 1919: 309-319.
- BAJPAI, S. and J. G. M. THEWISSEN. 1998. Middle Eocene cetaceans from the Harudi and Subathu formations of India. In J. G. M. Thewissen (ed.), *The Emergence of Whales Evolutionary Patterns in the Origin of Cetacea*, Plenum, New York, pp. 213-233
- , ———. 2000. A new diminutive Eocene whale from Kachchh (Gujarat, India) and its implications for locomotor evolution of cetaceans. *Current Science*, 79: 1478-1482.
- BANNERT, D., A. CHEEMA, A. AHMED, and U. SCHÄFFER. 1992. The structural development of the western fold belt, Pakistan. *Geologisches Jahrbuch, Hannover, Reihe B*, 80: 1-60 (with map in three sheets).
- BERGGREN, W. A. 1972. A Cenozoic time-scale -- some implications for regional geology and paleobiology. *Lethaia*, 5: 195-215.
- , D. V. KENT, C. C. SWISHER, and M.-P. AUBRY. 1995. A revised Cenozoic geochronology and chronostratigraphy. In W. A. Berggren, D. V. Kent, M.-P. Aubry, and J. A. Hardenbol (eds.), *Geochronology, Time Scales and Global Stratigraphic Correlations: A Unified Temporal Framework for an Historical Geology*, Society of Economic Paleontologists and Mineralogists, Special Volume, Tulsa, 54: 129-212.
- BISWAS, S. K. 1992. Tertiary stratigraphy of Kutch. *Journal of the Palaeontological Society of India*, 37: 1-29.
- EAMES, F. E. 1951. A contribution to the study of the Eocene in western Pakistan and western India. B. The description of the Lamellibranchia from standard sections in the Rakhi Nala and Zinda Pir areas of the western Punjab and in the Kohat District. *Philosophical Transactions of the Royal Society of London, Series B*, 235: 311-482.
- . 1952a. A contribution to the study of the Eocene in western Pakistan and western India. C. The description of the Scaphopoda and Gastropoda from standard sections in the Rakhi Nala and Zinda Pir areas of the western Punjab and in the Kohat District. *Philosophical Transactions of the Royal Society of London, Series B*, 236: 1-168.
- . 1952b. A contribution to the study of the Eocene in western Pakistan and western India: A. The geology of standard sections in the western Punjab and in the Kohat District. *Quarterly Journal of the Geological Society of London*, 107: 159-171.
- . 1952c. A contribution to the study of the Eocene in western Pakistan and western India: D. Discussion of the faunas of certain standard sections, and their bearing on the classification and correlation of the Eocene in western Pakistan and western India. *Quarterly Journal of the Geological Society of London*, 107: 173-196.
- FRAAS, E. 1904a. Neue Zeuglodonten aus dem unteren Mitteleocän vom Mokattam bei Cairo. *Geologische und Paläontologische Abhandlungen, Jena, Neue Folge*, 6: 197-220.
- . 1904b. Neue Zeuglodonten aus dem unteren Mitteleocän vom Mokattam bei Cairo. *Geologisches Zentralblatt, Leipzig*, 5: 374.
- GINGERICH, P. D. 1991. Partial skeleton of a new archaeocete from the earliest middle Eocene Habib Rahi limestone, Pakistan (abstract). *Journal of Vertebrate Paleontology*, 11A: 31.
- . 1998. Paleobiological perspectives on Mesonychia, Archaeoceti, and the origin of whales. In J. G. M. Thewissen (ed.), *The Emergence of Whales: Evolutionary Patterns in the Origin of Cetacea*, Plenum Publishing Corporation, New York, pp. 423-449.
- , M. ARIF, M. A. BHATTI, M. ANWAR, and W. J. SANDERS. 1997. *Basilosaurus drazindai* and *Basiloterus hussaini*, new Archaeoceti (Mammalia, Cetacea) from the middle Eocene Drazinda Formation, with a revised interpretation of ages of whale-bearing strata in the Kirthar Group of the Sulaiman Range, Punjab (Pakistan). *Contributions from the Museum of Paleontology, University of Michigan*, 30: 55-81.
- , ———, ———, and W. C. CLYDE. 1998. Middle Eocene stratigraphy and marine mammals (Cetacea and Sirenia) of the Sulaiman Range, Pakistan. *Bulletin of the Carnegie Museum of Natural History*, 34: 239-259.
- , ———, ———, H. A. RAZA, and S. M. RAZA. 1995b. *Protosiren* and *Babiacetes* (Mammalia, Sirenia and Cetacea) from the middle Eocene Drazinda Formation, Sulaiman Range, Punjab (Pakistan). *Contributions from the Museum of Paleontology, University of Michigan*, 29: 331-357.

- , ———, and W. C. CLYDE. 1995a. New archaeocetes (Mammalia, Cetacea) from the middle Eocene Domanda Formation of the Sulaiman Range, Punjab (Pakistan). *Contributions from the Museum of Paleontology, University of Michigan*, 29: 291-330.
- , S. M. RAZA, M. ARIF, M. ANWAR, and X. ZHOU. 1993. Partial skeletons of *Indocetus ramani* (Mammalia, Cetacea) from the lower middle Eocene Domanda Shale in the Sulaiman Range of Pakistan. *Contributions from the Museum of Paleontology, University of Michigan*, 28: 393-416.
- , ———, ———, ———, ———. 1994. New whale from the Eocene of Pakistan and the origin of cetacean swimming. *Nature*, 368: 844-847.
- , D. E. RUSSELL, D. SIGOGNEAU-RUSSELL, J.-L. HARTENBERGER, S. M. I. SHAH, M. HASSAN, K. D. ROSE, and R. H. ARDREY. 1979. Reconnaissance survey and vertebrate paleontology of some Paleocene and Eocene formations in Pakistan. *Contributions from the Museum of Paleontology, University of Michigan*, 25: 105-116.
- , B. H. SMITH, and E. L. SIMONS. 1990. Hind limbs of Eocene *Basilosaurus isis*: evidence of feet in whales. *Science*, 249: 154-157.
- and M. D. UHEN. 1996. *Ancalecetus simonsi*, a new dorudontine archaeocete (Mammalia, Cetacea) from the early late Eocene of Wadi Hitán, Egypt. *Contributions from the Museum of Paleontology, University of Michigan*, 29: 359-401.
- HARDENBOL, J. A. and W. A. BERGGREN. 1978. A new Paleogene numerical time scale. *American Association of Petroleum Geologists, Studies in Geology*, 6: 213-234.
- , J. THIERRY, M. B. FARLEY, T. JACQUIN, P.-C. D. GRACIANSKY, and P. R. VAIL. 1998. Mesozoic and Cenozoic sequence chronostratigraphic framework of European basins. In P.-C. d. Graciansky, J. A. Hardenbol, T. Jacquin, and P. R. Vail (eds.), *Mesozoic and Cenozoic Sequence Stratigraphy of European Basins*, SEPM Society for Sedimentary Geology, Special Publication 60, pp. 3-13 (eight charts).
- HARLAND, W. B., R. L. ARMSTRONG, A. V. COX, L. E. CRAIG, A. G. SMITH, and D. G. SMITH. 1990. *A Geologic Time Scale - 1989*. Cambridge University Press, Cambridge, 263 pp.
- , A. V. COX, P. G. LLEWELLYN, A. G. SMITH, and R. WALTERS. 1982. *A Geologic Time Scale*. Cambridge University Press, Cambridge, 131 pp.
- HEMPHILL, W. R. and A. H. KIDWAI. 1973. Stratigraphy of the Bannu and Dera Ismail Khan areas, Pakistan. U.S. Geological Survey Professional Paper, 716-B: 1-36.
- HULBERT, R. C. 1998. Postcranial osteology of the North American middle Eocene protocetid *Georgiacetus*. In J. G. M. Thewissen (ed.), *The Emergence of Whales: Evolutionary Patterns in the Origin of Cetacea*, Plenum Press, New York, pp. 235-267.
- , R. M. PETKEWICH, G. A. BISHOP, D. BUKRY, and D. P. ALESHIRE. 1998. A new middle Eocene protocetid whale (Mammalia: Cetacea: Archaeoceti) and associated biota from Georgia. *Journal of Paleontology*, 72: 907-927.
- JAFAR, S. A. and J. RAI. 1994. Late middle Eocene (Bartonian) calcareous nannofossils and its bearing on coeval post-trappean transgressive event in Kutch basin, western India. *Geophytology*, 24: 23-42.
- KÖTHE, A., A. M. KHAN, and M. ASHRAF. 1988. Biostratigraphy of the Surghar Range, Salt Range, Sulaiman Range and the Kohat area, Pakistan, according to Jurassic through Paleogene calcareous nannofossils and Paleogene dinoflagellates. *Geologisches Jahrbuch, Hannover, Reihe B*, 71: 1-87.
- KUMAR, K. and A. SAHNI. 1986. *Remingtonocetus harudiensis*, new combination, a middle Eocene archaeocete (Mammalia, Cetacea) from western Kutch, India. *Journal of Vertebrate Paleontology*, 6: 326-349.
- LA TOUCHE, T. D. 1893. Geology of the Sherani Hills. *Records of the Geological Survey of India*, 26 (3): 77-96, map, 5 plates.
- LATIF, M. A. 1964. Variations in abundance and morphology of pelagic Foraminifera in the Paleocene-Eocene of the Rakhri Nala, West Pakistan. *Geological Bulletin of Punjab University, Lahore*, 4: 29-100.
- MOHAN, M. and K. S. SOODAN. 1970. Middle Eocene planktonic foraminiferal zonation of Kutch, India. *Micropaleontology*, 16: 37-46.
- PATRIAT, P. and J. ACHACHE. 1984. India-Eurasia collision chronology has implications for crustal shortening and driving mechanism of plates. *Nature*, 311: 615-621.
- PILGRIM, G. E. 1940. Middle Eocene mammals from northwest India. *Proceedings of the Zoological Society of London, Series B*, 110: 127-152.
- SAHNI, A. 1981. Enamel ultrastructure of fossil Mammalia: Eocene Archaeoceti from Kutch. *Journal of the Palaeontological Society of India*, 25: 33-37.
- SAHNI, A. and V. P. MISHRA. 1972. A new species of *Protocetus* (Cetacea) from the middle Eocene of Kutch, western India. *Palaeontology*, 15: 490-495.
- . 1975. Lower Tertiary vertebrates from western India. *Monograph of the Paleontological Society of India*, 3: 1-48.

- SAMANTA, B. K. 1973. Planktonic Foraminifera from the Paleocene-Eocene succession in the Rakhi Nala, Sulaiman Range, Pakistan. *Bulletin of the British Museum (Natural History)*, Geology, 22: 421-482.
- SERRA-KIEL, J., L. HOTTINGER, E. CAUS, K. DROBNE, C. FERRÁNDEZ, A. K. JAUHRI, G. LESS, R. PAVLOVEC, J. PIGNATTI, J. M. SAMSO, H. SCHAUB, E. SIREL, A. STRUGO, Y. TAMBAREAU, J. TOSQUELLA, and E. ZAKREVSAYA. 1998. Larger foraminiferal biostratigraphy of the Tethyan Paleocene and Eocene. *Bulletin de la Société Géologique de France*, 169: 281-299.
- SHAH, S. M. I. 1977. Stratigraphy of Pakistan. *Memoirs of the Geological Survey of Pakistan*, 12: 1-138.
- . 1990. Coal resources of Balochistan, Pakistan. In A. H. Kazmi and R. A. Siddiqi (eds.), *Significance of the Coal Resources of Pakistan*, Geological Survey of Pakistan, Quetta, pp. 63-92.
- . 1991. Lithostratigraphic units of the Sulaiman and Kirthar Provinces, lower Indus Basin, Pakistan. *Geological Survey of Pakistan Information Release*, 519: 1-82.
- SIDDIQUI, Q. A. 1971. Early Tertiary Ostracoda of the family Trachyleberididae from West Pakistan. *Bulletin of the British Museum (Natural History)*, Geology Supplement 9, pp. 1-98.
- SINGH, P. and M. P. SINGH. 1991. Nannofloral biostratigraphy of the late middle Eocene strata of Kachchh region, Gujarat State, India. *Geoscience Journal*, 12: 17-51.
- TAINSH, H. R., K. V. STRINGER, and J. AZAD. 1959. Major gas fields of West Pakistan. *American Association of Petroleum Geologists Bulletin*, 43: 2675-2700.
- THEWISSEN, J. G. M. and S. T. HUSSAIN. 2000. *Attockicetus praecursor*, a new remingtonocetid cetacean from marine Eocene sediments of Pakistan. *Journal of Mammalian Evolution*, 7: 133-146.
- TOUMARKINE, M. and H. LUTERBACHER. 1985. Paleocene and Eocene planktic Foraminifera. In H. M. Bolli, J. B. Saunders, and K. Perch-Nielsen (eds.), *Plankton Stratigraphy*, Cambridge University Press, Cambridge, pp. 87-154.
- TRIVEDI, A. N. and P. P. SATSANGI. 1984. A new archaeocete (whale) from the Eocene of India. In N. A. Bogdanov (ed.), *Abstracts of 27th International Geological Congress, Moscow*, 1 pp. 322-323.
- UHEN, M. D. 1998. New protocetid (Mammalia, Cetacea) from the late middle Eocene Cook Mountain Formation of Louisiana. *Journal of Vertebrate Paleontology*, 18: 664-668.
- WARRAICH, M. Y., K. OGASAWARA, and H. NISHI. 2000. Late Paleocene to early Eocene planktic foraminiferal biostratigraphy of the Dungan Formation, Sulaiman Range, central Pakistan. *Paleontological Research*, Palaeontological Society of Japan, 4: 275-301.
- WELLS, N. A. 1984. Marine and continental sedimentation in the early Cenozoic Kohat Basin and adjacent northwestern Indo-Pakistan. Ph. D. dissertation, University of Michigan, Ann Arbor, 465.
- WILLIAMS, E. M. 1998. Synopsis of the earliest cetaceans: Pakicetidae, Ambulocetidae, Remingtonocetidae, and Protocetidae. In J. G. M. Thewissen (ed.), *The Emergence of Whales: Evolutionary Patterns in the Origin of Cetacea*, Plenum, New York, pp. 1-28.

APPENDIX

TABLE A-1 — Stratigraphic section of the Baska Formation measured November 22, 1999, in Chuk Dabh Janubi (starting at 30° 50.74' N, 70° 12.46' E; ending at 30° 50.77' N, 70° 12.82' E). Section is shown diagrammatically in Figure 3. Thicknesses were calculated and recorded to the nearest centimeter in the field, but are considered to have decimeter precision.

Bed thickness (m)	Cumulative thickness (m)	Lithological description
16.72	197.22	Gypsum, massive— top of BASKA FORMATION
2.65	180.50	Greenish gray shale
1.30	177.85	Thin-bedded brown limestone
4.26	176.55	Brown shale
5.30	172.29	Gypsum, massive
4.56	166.99	Yellowish gray shale, mostly covered
0.15	162.43	Yellow marl
1.40	162.28	Yellowish brown shale
0.20	160.88	Brown platy limestone
1.23	160.68	Yellowish brown shale

2.70	159.45	Gypsum, massive
2.50	156.75	Yellowish brown shales
4.50	154.25	Gypsum, massive
4.86	149.75	Yellowish gray shales, mostly covered
0.23	144.89	Gypsum
0.20	144.66	Light brown limestone, thinly-bedded, wave-rippled
3.04	144.46	Yellowish gray shales, mostly covered
1.08	141.42	Gypsum
0.30	140.34	Limestone, gray, hard, compact
4.00	140.04	Yellowish gray blocky shales with marls
0.15	136.04	Marl packed with shell fragments
0.20	135.89	Shale
0.65	135.69	Limestone, hard, compact, thin- to medium-bedded
2.50	135.04	Shale, light yellowish gray, mostly covered
0.35	132.54	Sugary-textured limestone
0.65	132.19	Shale, light yellowish gray, mostly covered
1.80	131.54	Thinly-bedded, rubbly, light yellowish gray bioclastic marl
1.65	129.74	Gypsum
0.58	128.09	Laminated brown limestone with white gypsum inclusions
5.83	127.51	Greenish gray shale, mostly covered
0.20	121.68	Gypsum at base to limestone at top
2.60	121.48	Greenish-gray shale to marl
1.10	118.88	Gypsum with 20 cm limestone at base
1.50	117.78	Green to gray shales and marls
1.10	116.28	Gypsum
1.70	115.18	Green shales with <i>Stephanodus</i> tooth
0.40	113.48	Brownish gray massive limestone, hard, rippled top, wavy bedding
1.80	113.08	Pale yellowish brown limestone [10YR6/2]
0.50	111.28	Yellowish marly limestone, occasional shell fragments
1.55	110.78	Light yellowish gray shales, mostly covered
0.80	109.23	Gypsum, some with small ripple marks
0.20	108.43	Limestone
0.56	108.23	Yellowish gray shales, mostly covered
1.50	107.67	Gypsum, massive, with low-angled scour base
1.04	106.17	Light yellowish gray shales with elongated calcite nodules
0.60	105.13	Limestone with gypsum masses and pinkish porous top (weathered?)
1.80	104.53	Green to yellowish shale
0.65	102.73	Gypsum, greenish brown, basal part impure, middle massive, top shaly
1.20	102.08	Blocky shale, light yellowish gray
0.40	100.88	Marly limestone over marl
3.64	100.48	Light gray shale
0.15	96.84	Clastic bed with rock fragments, carbonaceous material, shell fragments
0.60	96.69	Yellowish brown shales
0.80	96.09	Brown-tan-brown limestone
0.80	95.29	Light gray shales
0.50	94.49	Sugary-textured platy limestone
4.66	93.99	Light gray shales, weather to light yellowish gray
0.70	89.33	Medium-bedded limestone
11.20	88.63	Alternating calcareous fissile shales and shelly marl beds
0.40	77.43	Marly limestone
12.66	77.03	Marly limestones in shales, partly covered
0.25	64.37	Light gray limestone, compact and hard, rectangular jointing
7.70	64.12	Yellowish brown 10-20 cm shelly marls interbedded with gray-green shales
1.00	56.42	Medium gray limestone, massive and hard, with burrowed top
1.70	55.42	Yellowish gray shale with thin marly intercalations
0.60	53.72	Medium gray massive limestone
5.56	53.12	Marls and limestones with mollusks, including 40 cm massive limestone
0.35	47.56	Mollusk-packed marl
6.08	47.21	Marls and limestones, minor shales

13.68	41.13	Alternating yellowish shales, marls, and occasional marly limestones
2.80	27.45	Grayish red shale [5R4/2], mottled with green
2.10	24.65	Greenish gray shale, marl at top with oyster shell fragments
1.20	22.55	Oyster zone with 40 cm oyster coquina near top
2.60	21.35	Gray shale
3.00	18.75	Yellow marly limestones alternating with tan shales
0.20	15.75	Ferruginous platy bioclastic limestone
0.30	15.55	Tan shale
0.80	15.25	Tan marly limestone
4.63	14.45	Green and dark gray shales
9.82	9.82	Tan marly oyster limestone, alternating with tan shales— base of BASKA FORMATION

TABLE A-2 — Stratigraphic section of the Habib Rahi Formation measured November 22, 1999, in Chuk Dabh Janubi (at 30° 50.77' N, 70° 12.82' E). Section is shown diagrammatically in Figure 6. Thicknesses were calculated and recorded to the nearest centimeter in the field, but are considered to have decimeter precision.

Bed thickness (m)	Cumulative thickness (m)	Lithological description
9.62	62.11	Thin marls alternating with brown shales— top of HABIB RAHI FORMATION
9.12	52.49	Platy 10 cm marls alternating with 40 cm brown shales
7.60	43.37	Platy 15 cm limestones with chert, alternating with marl and shale
10.64	35.77	Platy 30 cm marls alternating with 20 cm blocky shales
0.50	25.13	Gray shales
0.25	24.63	Marl with many ferruginous assilines
6.08	24.38	Blue-gray shales
0.30	18.30	Blue-gray blocky marl
1.20	18.00	Blue-gray shale
0.60	16.80	Blue-gray blocky marl with assilines
16.20	16.20	Green and yellowish green shales— base of HABIB RAHI FORMATION

TABLE A-3 — Stratigraphic section of the Domanda Formation measured November 23 and 24, 1999, just north of Zuli Khan Sham (starting at 30° 53.27' N, 70° 13.23' E; ending at approximately 30° 53.20' N, 70° 13.60' E; details at top of section are from nala cutting at 30° 53.82' N, 70° 13.76' E). Section is shown diagrammatically in Figure 6. Thicknesses were calculated and recorded to the nearest centimeter in the field, but are considered to have decimeter precision.

Bed thickness (m)	Cumulative thickness (m)	Lithological description
9.12	366.36	Green shale with occasional oyster-packed bed; upper 2.75 m is <i>Alveolina-Nummulites-Discocyclina</i> -packed; top is highly burrowed— top of DOMANDA FORMATION
5.60	357.24	Zone of yellowish gray to brownish gray with minor greenish gray fissile shale
1.50	351.64	Yellowish gray fissile shale with rare bivalves, weathers maroon
3.75	350.14	Yellowish gray fissile shale zone with some light brownish gray shale, weathers brownish gray
0.50	346.39	Dark greenish gray [5GY4/1] fissile shales with brownish gray partings [5YR4/1]
0.30	345.89	Greenish gray [5GY6/1] <i>Alveolina</i> bed with limestone concretions that include planktonic forams

3.64	345.59	Green fissile shales
12.90	341.95	Red-brown fissile shales
1.30	329.05	Yellowish zone
4.56	327.75	Red-brown fissile shales
3.04	323.19	Zone of red-purple oxides on surface; fresh color is grayish red [10R4/2] or moderate brown [5YR4/4]
6.64	320.15	Red-brown fissile shales
4.00	313.51	Green and gray shales with alternation of olive brown shales
0.15	309.51	Bivalve-filled rubbly marl, fish bones, oysters; level of most <i>Qaisracetus</i> specimens
4.40	309.36	Green shales with shell bed ca. 10 cm thick 2.5 m below top
0.30	304.96	Brown hard blocky oyster limestone, oysters richest at base— 'wavy limestone'
4.90	304.66	Light green shales; level of type specimen of <i>Qaisracetus spinalis</i>
0.20	299.76	Yellow shale with white shell endocasts
3.56	299.56	Green shales with thin maroon-colored bed
7.60	296.00	Green shales
3.80	288.40	Red and yellow shales
4.80	284.60	Grayish red [10R4/2] to pale brown [5YR5/2] fissile shale, weathers to maroon and brown
5.35	279.80	Brown fissile shale
0.30	274.45	<i>Turritella</i> and oyster-packed 8 cm marl at top of shell-rich shale; includes slab with tiny bivalves
19.76	274.15	Alternation of dark yellowish brown [10YR4/2] and green blocky shales
6.08	254.39	Gray-green multani (fuller's earth), weathering light brown
0.10	248.31	Zone with crab burrows, some ooid-filled
2.00	248.21	Gray-green multani (fuller's earth), weathering light brown
0.10	246.21	Shell bed with some carbonate concretions, sulphurous at top
2.25	246.11	Gray green multani (fuller's earth), weathering light brown
0.10	243.86	Shell bed
17.48	243.76	Gray-green light multani (fuller's earth), some lighter and darker beds
0.20	226.28	Zone of three thin centimeter-scale limestones separated by shales
4.56	226.08	Gray-green fissile shales
0.35	221.52	Dark olive green shale, with sulphurous concretion at top
2.10	221.17	Gray green light multani (fuller's earth) weathering light brown
0.10	219.07	Bivalve shell bed
17.48	218.97	Olive gray shales with thin marl beds, light-gray multani (fuller's earth), sulphurous mounds
0.10	201.49	Thinly-bedded, half-centimeter scale platy limestone, ridge-forming
12.66	201.39	Light olive green shale
9.12	188.73	Multani (fuller's earth) as below; dark gray shale 3 m from top of unit
1.00	179.61	Brown clay shale, blocky, dark yellowish brown [10YR4/2]
12.16	178.61	Light olive gray fissile shale
7.60	166.45	Multani (fuller's earth) with gray alternations as below; discontinuous 20 cm brown marl at top
1.80	158.85	Zone with papery fissile shale at bottom and top, 25 cm brown-weathering laminated marl in middle
10.64	157.05	Multani (fuller's earth) with gray alternations as below
0.70	146.41	Zone with marl beds at bottom and top, shale between is multani (fuller's earth) with red partings
7.35	145.71	Multani (fuller's earth) alternating with meter-scale beds every few meters that lack red partings
0.03	138.36	Marl, dark brown
4.86	138.33	Multani (fuller's earth) clay shale, fissile, light olive gray [5Y6/1] with dark reddish brown [10R3/4] partings, fish coprolites; surface weathers orange-brown
12.16	133.47	Monotonous fissile shale, light olive gray [5Y5/2], weathers to light greenish gray [5G8/1]
0.40	121.31	Zone with thin yellowish brown marls at bottom and top; olive shale between
7.50	120.91	Light olive gray to greenish gray shale with occasional dewatering mounds
0.25	113.41	Yellowish brown marl, with flower-like circular dewatering structure (photo)
3.95	113.16	Olive gray to greenish gray shale with dewatering mound
0.70	109.21	Yellowish brown marl at bottom and top, yellowish brown shale in middle
7.30	108.51	Light olive gray [5Y5/2] fissile shale at base, greenish gray [5GY6/1] at top

0.15	101.21	Yellowish brown marl bed, wavy dewatering mound on top
11.64	101.06	Alternations of dark yellowish brown and light olive shale
0.20	89.42	Lenticular marl concretion zone
15.40	89.22	Alternations of dark yellowish brown [10YR4/2] with light olive gray [5Y6/1] fissile shale; former weathers to green and latter to light gray
0.20	73.82	Lenticular marl concretion zone
35.72	73.62	Alternations of dark yellowish brown [10YR4/2] with light olive gray [5Y6/1] fissile shale
0.30	37.90	Centimeter-scale beds of tan marl
9.12	37.60	Fissile gray shales with few or no marl beds
0.60	28.48	Fissile dark gray shales
5.60	27.88	Blue-gray shales with centimeter scale marls
13.68	22.28	Blue-gray shales with 1-3 cm interbeds of marl
1.20	8.60	Three thick tan marly limestone beds separated by gray blocky shale
7.40	7.40	Fissile gray-brown shale with 2-5 cm plates of marly limestone spaced every 50 to 100 cm— base of DOMANDA FORMATION

TABLE A-4 — Stratigraphic section of the Pir Koh Formation measured November 24, 1999, in Baher Dabh Shumali at 30° 53.82' N, 70° 13.76' E. Section is shown diagrammatically in Figure 9. Thicknesses were calculated and recorded to the nearest centimeter in the field, but are considered to have decimeter precision.

Bed thickness (m)	Cumulative thickness (m)	Lithological description
7.08	19.39	Gray shale and marl; color is light olive gray [5Y6/1], weathers to light bluish gray— top of PIR KOH FORMATION
4.82	12.31	Marl, generally massive but weathering into laminae
1.15	7.49	Shale and thinly laminated marl
0.25	6.34	Marl
0.06	6.09	Shales
0.18	6.03	Marl
0.10	5.85	Shales
0.22	5.75	Marl
0.21	5.53	Marly shales
0.50	5.32	Marl packed with <i>Discocyclus</i>
0.25	4.82	Shales
0.50	4.57	Marl
0.40	4.07	Shales
0.70	3.67	Marl
0.40	2.97	Shales
0.45	2.57	Marl
0.30	2.12	Shale and marl, greenish gray
1.82	1.82	Thick blocky or nodular marl, highly burrowed, hummocky base, very light gray color [N8], weathers light greenish gray [5GY8/1]— base of PIR KOH FORMATION

TABLE A-5 — Stratigraphic section of the Drazinda Formation measured November 24, 1999, in Baher Dabh Shumali. First part of section started at 30° 53.82' N, 70° 13.76' E, and ended at the *Discocyclus* marker bed at 30° 53.77' N, 70° 13.96' E. Second part of section started at the *Discocyclus* marker bed at 30° 53.41' N, 70° 13.90' E, and ended at 30° 53.31' N, 70° 14.14' E. Basal 6 m of Chitarwata Formation is included to document the transition to coarser clastics. Section is shown diagrammatically in Figure 9. Thicknesses were calculated and recorded to the nearest centimeter in the field, but are considered to have decimeter precision.

Bed thickness (m)	Cumulative thickness (m)	Lithological description
0.80	6.05	Yellow clay shale zone with black weathered nodules [reworked from Drazinda Fm.?]]
0.60	5.25	Gray shales
0.60	4.65	Yellow siltstone
0.75	4.05	Very fine-grained sandstone
0.70	3.30	Yellow shales
2.60	2.60	Gray silty shale with red mottling— base of CHITARWATA FORMATION
0.25	434.26	Moderate red clay [5R4/6]— top of DRAZINDA FORMATION
2.50	434.01	Dark yellowish orange shale [10YR6/6]
31.92	431.51	Dark yellowish brown shale [10YR4/2] with gastropods and bivalves
15.20	399.59	Olive gray [5Y4/1] fissile shale
12.16	384.39	Light greenish gray [5G8/1] fissile shale
0.40	372.23	Hard gray marl bed, weathers yellow
16.72	371.83	Reddish brown shales
13.68	355.11	Green shales
6.08	341.43	Maroon shales
3.00	335.35	Green shales with very small <i>Discocyclus</i> at base
21.28	332.35	Maroon and brown shale alternations
1.25	311.07	Green fossiliferous shale with cup corals
7.60	309.82	Reddish brown shales
16.72	302.22	Green shales with occasional bivalves
1.50	285.50	Brown shales
0.40	284.00	Green shale with bivalve hash at base, bryozoans
38.00	283.60	Yellowish brown to reddish shales with large dark concretions, weathers dark reddish brown [10R3/4]
1.70	245.60	Green shales, weather yellow
1.50	243.90	Maroon shales
0.20	242.40	Light green shales with <i>Turritella</i>
11.64	242.20	Reddish brown shales
1.00	230.56	Gray shale
1.00	229.56	Red shale
2.50	228.56	Olive green shale
0.10	226.06	Shell bed with <i>Turritella</i>
19.76	225.96	Dark gray-green unit with occasional <i>Protosiren sattaensis</i> vertebrae, <i>Conus colossus</i>
3.04	206.20	Dusky yellow shales [5Y6/4]
39.52	203.16	Light olive gray [5Y5/2] fissile shales
0.70	163.64	<i>Discocyclus</i> marker bed, packed with <i>Discocyclus sowerbyi</i> ; limestone at base
8.70	162.94	Green shales
0.10	154.24	Limestone packstone with <i>Turritella</i> and <i>Discocyclus</i> , including <i>Discocyclus sowerbyi</i> fragments
9.12	154.14	Reddish brown shales, some green shale at top
0.10	145.02	Limestone coquina with <i>Nummulites beaumonti</i> as below
13.68	144.92	Reddish brown shales
0.10	131.24	Limestone coquina with 2 cm and 6 cm flattened crab burrows filled with nummulites; <i>Nummulites beaumonti</i> common; rare oyster shells; forms dip slopes
1.50	131.14	Reddish brown shales
2.50	129.64	Reddish brown shales with 1 cm limestone coquina at top

2.25	127.14	Reddish brown shales with 1 cm limestone coquina at top
1.35	124.89	Reddish brown shales with 1 cm limestone coquina at top
2.85	123.54	Reddish brown shales with 1 cm limestone coquina at top
1.00	120.69	Reddish brown shales with 1 cm limestone coquina at top
7.60	119.69	Reddish brown shales with 1 cm limestone coquina at top
0.15	112.09	Laminated limestone with bryozoans
9.12	111.94	Reddish brown shale
1.25	102.82	Yellowish gray shale with thin marl unit
9.85	101.57	Brown fissile shales
1.25	91.72	Green shales with rare bivalves
10.64	90.47	Zone of green shales with <i>Discocyclus</i> at base, brown shales in middle and at top
6.08	79.83	Brown-gray alternating fissile shales
38.00	73.75	Dusky yellow to yellowish gray shales
9.12	35.75	Greenish gray [5GY6/1] fissile shales
18.24	26.63	Dusky yellow [5Y6/4] to yellowish gray [5Y7/2 or 5Y8/1] blocky to laminated clay shale
5.35	8.39	Blue-gray fissile shales
0.30	3.04	Marly gray shale, forms dip slope
2.74	2.74	Light gray-green fissile shales— base of DRAZINDA FORMATION
